SYNTHESIS AND CHARACTERIZATION OF BONE CEMENT BASED ON NEW BIOACTIVE GLASS CERAMIC WITH PMMA MATERIALS

2023
MASTER THESIS
METALLURGICAL AND MATERIALS ENGINEERING

Anmar Fouad Kadhim IBADI

Thesis Advisor
Assist. Prof. Dr. Alper İNCESU

SYNTHESIS AND CHARACTERIZATION OF BONE CEMENT BASED ON NEW BIOACTIVE GLASS CERAMIC WITH PMMA MATERIALS

Anmar Fouad Kadhim IBADI

Thesis Advisor
Assist. Prof. Dr. Alper İNCESU

T.C.
Karabük Üniversitesi
Institute of Graduate Programs
Department of Metallurgical and Materials Engineering
Prepared as
Master Thesis

KARABÜK
July 2023

I certify that in my opinion the thesis submitted by Anmar Fouad Kadhim IBADI titled “SYNTHESIS AND CHARACTERIZATION OF BONE CEMENT BASED ON NEW BIOACTIVE GLASS CERAMIC WITH PMMA MATERIALS” is fully adequate in scope and in quality as a thesis for the degree of Master of Science

Assist. Prof. Dr. Alper İNCESU .....
Thesis Advisor, Department of Metallurgical and Materials Engineering

This thesis is accepted by the examining committee with a unanimous vote in the Department of Metallurgical and Materials Engineering as a Master of Science thesis. July 24 , 2023

Examining Committee Members (Institutions) Signature

Chairman: Assoc. Prof. Dr. Yüksel AKINAY (YYU) .....

Member : Assist. Prof. Dr. Yasin AKGÜL (KBU) .....

Member : Assist. Prof. Dr. Alper İNCESU (KBU) .....

The degree of Master of Science by the thesis submitted is approved by the Administrative Board of the Institute of Graduate Programs, Karabuk University.

Prof. Dr. Müslüm KUZU .....
Lisansüstü Eğitim Enstitüsü Müdürü

"I declare that all the information within this thesis has been gathered and presented in accordance with academic regulations and ethical principles and I have according to the requirements of these regulations and principles cited all those which do not originate in this work as well."

Anmar Fouad Kadhim IBADI

ABSTRACT

Master Thesis

SYNTHESIS AND CHARACTERIZATION OF BONE CEMENT BASED ON NEW BIOACTIVE GLASS CERAMIC WITH PMMA MATERIALS

Anmar Fouad Kadhim IBADI

Karabük University
Institute of Graduate Programs
The Department of Metallurgical and Materials Engineering

Thesis Advisor:
Assist. Prof. Dr. Alper İNCESU
July 2023, 87 pages

Synthesis and characterization of modified 45S5 bioglass ceramic analogues with varying concentrations of V_2O_5. The bioglass compositions, including SiO_2, CaO, NaO, P_2O_5, B_2O_3, and V2O5. The V_2O_5 was added using a melt-quenching technique, resulting in different compositions labelled NCSB(X)V, where X represents the weight percentage of V_2O_5 (1%, 3%, and 5%). The mixture of oxides and V_2O_5 was melted in an electric furnace at 1100 ℃ for 2 hours, then cooling in distilled water. The resulting powders were milled, sintered at 800 °C for four hours, and analyzed using X-ray diffractometry. Sintering was essential to obtain an amorphous material. The ground sintered bioglass ceramics were produced using a rotary mill, and a TG/DTA analysis was conducted to determine the glass transition temperature (Tg), the temperature at which crystallization began (Tc onset), and the temperature at which it peaked (Tc).

The result shows that after 7 days of immersion, two new apatite peaks appeared, and after 14 days, all peaks became identical, indicating good crystalline phase formation. The presence of V_2O_5 affected the crystal size and lattice strain, resulting in broader XRD patterns. V_2O_5 hindered the formation of large apatite crystals and promoted the agglomeration of amorphous calcium phosphate. The combination of apatite with boron resulted in increased lattice constants due to calcium's smaller ionic radius than boron. XRD patterns and FTIR spectra confirmed the formation of low-crystallinity calcium phosphate crystals. The formation of hydroxyapatite (HA) and hydroxyapatite cluster (HCA) crystals on the surfaces of bioactive glass ceramics. SEM and EDX analysis showed that HA formation initiated on day 3, while HCA cluster crystals started forming on day 21. The dissolution process decreased sample weight as Ca2+ and PO43- ions were released from the glass matrix into the surrounding simulated body fluid (SBF) solution. It was hypothesized that an intermediate vanadium ion played a role in loosening the borosilicate glass network by forming BO3 groups in a triangular shape. At different stages, C-O and P-O functional groups facilitated the formation of HCA layers. Based on these findings, bioactive glass ceramics containing borate and V_2O_5 are considered promising materials for medical applications. Commercial PMMA bone cement is modified by incorporating varying filler loadings of synthesized glass-ceramic. The study investigated the effect of filler content on the setting and handling properties of bone cement. As the amount of filler increased, the peak temperature during the setting reaction decreased, and all filled bone cement samples exhibited lower peak temperatures compared to the control (unfilled) sample. However, no clear trend was observed in the setting time with increased filler loads. On the other hand, the dough time decreased with increased filler loading. Based on the findings, it was concluded that bone cement containing 10 and 20 wt% glass-ceramic filler loading demonstrated optimal setting and handling properties.

Key Word **:** Glass-ceramic, Melt-quenching, Bioactivity, Bone cement, PMMA, Mechanical properties, Setting time

Science Code : 91501

ÖZET

Yüksek Lisans Tezi

PMMA MALZEMELERİ İLE YENİ BİYOAKTİF CAM SERAMİK ESASLI KEMİK ÇİMENTOSUNUN SENTEZİ VE KARAKTERİZASYONU

Anmar Fouad Kadhim IBADI

Karabük Üniversitesi
Fen Bilimleri Enstitüsü
Metalurji ve Malzeme Mühendisliği

Tez Danışmanı:
Assist. Prof. Dr. Alper İNCESU
Temmuz 2023, 87 sayfa

Değişken konsantrasyonlarda V_2O_5 ile değiştirilmiş 45S5 biyocam seramik analoglarının sentezi ve karakterizasyonu. SiO_2, CaO, NaO, P_2O_5, B2O3 ve V_2O_5 dahil biyocam bileşimleri. V_2O_5, eriterek söndürme tekniği kullanılarak ilave edildi ve NCSB(X)V olarak etiketlenen farklı bileşimler elde edildi; burada X, V_2O_5 'in ağırlık yüzdesini (%1, %3 ve %5) temsil eder. Oksitler ve V_2O_5 karışımı elektrikli bir fırında 1100 ℃'de 2 saat eritildi, ardından damıtılmış suda soğutuldu. Nihai tozlar öğütüldü, 800 °C'de dört saat sinterlendi ve X-ışını difraktometrisi kullanılarak analiz edildi. Amorf bir malzeme elde etmek için sinterleme esastır. Öğütülmüş sinterlenmiş biyocam seramikler bir döner değirmen kullanılarak üretildi ve cam geçiş sıcaklığını (Tg), kristalleşmenin başladığı sıcaklığı (Tc başlangıcı) ve zirve yaptığı sıcaklığı (Tc) belirlemek için bir TG/DTA analizi yapıldı.).

Sonuç, 7 günlük daldırmadan sonra iki yeni apatit pikinin ortaya çıktığını ve 14 gün sonra tüm piklerin aynı hale geldiğini ve iyi bir kristal faz oluşumuna işaret ettiğini

gösterir. V_2O_5 'in varlığı, kristal boyutunu ve kafes gerilimini etkileyerek daha geniş XRD modelleriyle sonuçlandı. V_2O_5, büyük apatit kristallerinin oluşumunu engelledi ve amorf kalsiyum fosfatın topaklanmasını destekledi. Apatitin bor ile kombinasyonu, kalsiyumun bordan daha küçük iyonik yarıçapına bağlı olarak kafes sabitlerinin artmasına neden oldu. XRD desenleri ve FTIR spektrumları, düşük kristallikte kalsiyum fosfat kristallerinin oluşumunu doğruladı. Biyoaktif cam seramiklerin yüzeylerinde hidroksiapatit (HA) ve hidroksiapatit kümesi (HCA) kristallerinin oluşumu. SEM ve EDX analizi, HA oluşumunun 3. günde başladığını, HCA küme kristallerinin ise 21. günde oluşmaya başladığını gösterdi. Çözünme işlemi, Ca2+ ve PO43- iyonları cam matristen çevredeki simüle edilmiş vücut sıvısına (SBF) salındıkça numune ağırlığını düşürdü. çözüm. Bir ara vanadyum iyonunun, üçgen şeklinde BO3 grupları oluşturarak borosilikat cam ağının gevşemesinde rol oynadığı varsayılmıştır. Farklı aşamalarda, C-O ve P-O fonksiyonel grupları, HCA katmanlarının oluşumunu kolaylaştırdı. Bu bulgulara dayanarak, borat ve V_2O_5 içeren biyoaktif cam seramikler, tıbbi uygulamalar için umut verici malzemeler olarak kabul edilmektedir. Ticari PMMA kemik çimentosu, sentezlenmiş cam seramiğin değişen dolgu yükleri dahil edilerek modifiye edilir. Çalışma, dolgu içeriğinin kemik çimentosunun sertleşme ve işleme özellikleri üzerindeki etkisini araştırmıştır. Dolgu maddesi miktarı arttıkça, sertleşme reaksiyonu sırasında pik sıcaklık azaldı ve tüm doldurulmuş kemik çimentosu numuneleri, kontrol (doldurulmamış) numuneye kıyasla daha düşük pik sıcaklıklar sergiledi. Ancak artan dolgu yükleri ile priz süresinde net bir eğilim gözlenmemiştir. Diğer taraftan dolgu yüklemesi arttıkça hamur süresi kısalmıştır. Bulgulara dayanarak, ağırlıkça %10 ve %20 cam-seramik dolgu yükü içeren kemik çimentosunun optimum ayar ve kullanım özellikleri gösterdiği sonucuna varılmıştır.

Anahtar Sözcükler : Cam-seramik, Melt-söndürme, Biyoaktivite, Kemik çimentosu, PMMA, Mekanik özellikler, Sertleşme süresi

Bilim Kodu : 91501

ACKNOWLEDGMENT

Firstly I thank Allah who knows all, rules all and sees all for granting me this victory and desire to achieve this study. I would especially like to express my deep appreciation and sincere thanks to my manager's assistant. Prof. Dr. Alper İNCESU for their patience, attention, understanding and balance in carrying out the activities throughout the work, accompanying, instructing and teaching at every step with full commitment. I would like to thank the reviewer in advance. We thank the committee members for their willingness to contribute actively to this work. My parents for all their hard work in life. To my family and friends for their constant care. And I thank Scientific Research Projects Coordination Unit of Karabuk University. Project Number: KBUBAP-22-YL-136.

CONTENTS

Page

Page

Page

LIST OF FIGURES

Page

LIST OF TABLES

Page

SYMBOLS AND ABBREVIATIONS INDEX

SYMBOLS

ºC : The degree Celsius

2θ : The diffraction angle

λ : wavelength of the X-ray

E : Young's modulus

σc : compressive strength

I_B : Bioactivity index

ABBREVIATIONS

HA : Hydroxyapatite

RT : Room Temperature

JCPDS : Joint Committee for Powder Diffraction Standards

PMMA : Poly Methyl Methacrylate

MMA : Methyl Methacrylate

BG : Bioactive glass

ASTM : American Society for Testing and Materials

PART 1

INTRODUCTION

1.1.INTRODUCTION

Skeletal system; It is the system that sustains our body, enables us to move, protects our internal organs against external impacts and gives our body its shape. Injuries caused by various reasons in our skeletal system can pose significant problems for our body. Non-serious injuries to the bone structure can be healed quickly by the mechanism of the bone system. However, particular interventions, such as biomaterials, may be needed in severe injuries [1]. Biomaterial is a material that can be used to replace damaged tissues or organs in the human body, meet its functions and be accepted by the body without any problems [2]. The use of biomaterials began in ancient times. The artificial eyes, noses and teeth found in Egyptian mummies are the best examples. While the use of gold in dentistry dates back to 2000 years ago, bronze and copper bone implants date back to BC [3].

Biomaterials are used in the body under variable environmental conditions. For this reason, biomaterials must have specific properties to be used in the body. One of the most essential features that biomaterials should have is that they do not cause side effects and can adapt when interacting with biological systems. Orthopedic materials are exposed to millions of loading cycles during movement. For this reason, the mechanical and fatigue strength properties of the biomaterial used in orthopedic applications are significant. In addition, since the human body contains protein-oxygenated salt solutions, these materials must have many properties, such as high corrosion resistance, non-deformation, and non-carcinogenic and toxic effects [4]. However, today, expectations from such materials have increased, and when bone tissue is damaged or lost, it has become one of today's essential medical and social needs to be able to produce artificial bone tissue to be used in the repair or

Complete regeneration of the damaged area. One of the most essential options for artificial bone production today is bone tissue engineering. The aim of bone tissue engineering, which eliminates the need for permanent implants, is To provide bone regeneration by using a tissue scaffold that resembles bone structure, can be attached to bone and provides bone development [5].

Bone grafts are frequently used to reconstruct bone trauma, bone infections, congenital anomalies, tumour excision, and defects that will occur in revision arthroplasty surgery to benefit from their supportive and bone formation stimulating effects [6, 7]. The regeneration capacity of bone tissue is relatively high. Bone tissue can completely restore its original structure and function. If the resulting bone defects are minor, graft application may not be necessary since the bone can heal spontaneously thanks to the regeneration feature of the tissue [8]. The need for graft materials depends on the size of the bone defects. The slightest bone defect above a specific size that cannot heal spontaneously during the organism's lifetime is called Critical Size Bone Defect (CBD). In significant defects and severe loss of bone volume, the bone cannot heal independently. In critically sized bone defects, grafting will be required for the bone to maintain its function [9]. Although many alternative methods are used to reconstruct bone defects, the ideal method is to reconstruct the defect with another bone tissue with similar size, shape and antigenically similar properties.

The grafts used to repair bone defects are autogenous, allogeneic and xenogenous grafts. An ideal bone graft should have at least one of the functions of osteointegration, osteoinduction, osteoconduction and osteogenesis [10]. Despite the benefits of autogenous, allogeneic and xenogenous grafts, the disadvantages of each have led to the search for alternatives. Bioceramics in alloplasts (biomaterials), which are materials that can replace bone, are widely used in orthopedics and dentistry[11]. The need for such materials in veterinary medicine is increasing daily. The classification of bone substitute materials is given in Table 1 [12, 13].

Table 1.1 Classification of bone substitute materials [12, 13].

Tissue origins	**polymers**	**calcium sulphate**	**Bioceramic**
Dentine cement Cartilage Sclera Durameter Others	Polymethylmethacrylate Proplast	Plaster of Paris cap set	Tricalcium phosphate Hydroxyapatite Bioactive glasses

Biomaterials, graft types obtained from inert synthetic materials and sometimes called implant materials, are generally used to initiate osteogenesis and accelerate bone defect healing [14]. Biomaterials provide bone formation by creating a distinct biological response at the interface with bone. Biomaterials are divided into 4 groups: ceramics, metals, polymers and composites. The osteogenic and osteoconductive properties of these materials have been determined. An ideal synthetic graft should provide bone formation with an osteoconductive matrix structure that will provide a suitable environment for osteoprogenitor cells to settle and develop. Bioceramics for bone repair are the materials most subject to biomaterial studies today. Biomaterials have become materials that can be used safely due to their advantages, such as no risk of disease transmission, easy application, short operation time, no need for a donor site, and various sizes and shapes in graft materials. Bioceramics, which are considered among alternative materials instead of bone grafts, are challenging but brittle materials that are highly resistant to pressure, biocompatible, and extremely resistant to abrasion, although they have a slight shrinkage feature. Bioceramics are among the most promising biomaterials among other graft materials in replacement applications [15, 16].

Bioactive glasses, which are classified as bioceramics, consist of silicon dioxide (45%), calcium oxide (24.5%), sodium dioxide (24.5%) and phosphorus oxide (6%)

[17]. All these elements are naturally present in the body. The binding of bioactive glasses to bone tissue with organic bonds, having enzymatic activities, contributing to the formation of vascular structure, and supporting the differentiation of mesenchymal cells in bone tissue are among the most important features [18].

Bioactive glasses can form a chemical bond between the bone and the implant. The main difference distinguishing bioactive glasses from other natural and synthetic bioceramics is their chemical properties, and their binding to tissues can be controlled [19]. Bioactive glass, which is a synthetic material, is chemically bonded to the bone tissue, and new bone formation occurs thanks to the collagen, ground substance and matrix vesicles provided by osteoblasts for primary mineralization on this bonding surface. Another distinctive feature of bioactive glasses is that in cases of breakage during the application if the pieces are not separated from each other, they can recombine thanks to the self-repairing capacity of the surface apatite layer. Bioactive glass is osteoconductive; when it comes into contact with a bone-forming cell, bone is formed there. Bone formation is observed on the entire surface of the bioactive glass, not just where it comes into contact with the bone. In addition, bioactive glass is a synthetic material that strengthens the regeneration abilities of tissues [20]. Bioactive glasses form hydroxyapatite in cell culture studies and in vivo applications and provide bone-implant connection. In addition, it is thought that the positive contribution of bioactive glasses to bone formation is due to their increase in collagen synthesis and cross-linking rate [21]. All of the tissue repaired with bioactive glass has transformed into bone tissue, and it has been reported that it does not consist of a mixture of material and bone as in other bone substitute materials [22].

1.2.OBJECTIVE OF THE WORK

The need to develop materials that replace bone parts without harming the individual has been demanded for years, and many studies are being carried out in this area. Many materials can have this type of use, but to be used in this way, these materials need to have characteristics compatible with those of organisms.

In this study, Based on the SiO_2-Na_2O-P_2O_5-CaO bioactive glass system, where the effect of 15% boron and vanadium oxides addition at four different rates (X% V_2O_5

(X = 1, 3, and 5).) on the bioactivity properties was investigated. Bioactive glasses were produced using the melting method and used for cement production. The production of bone cement based on PMMA as a matrix and the addition of different concentrations of bioactive glass. Structural and physical properties were determined by applying various characterization methods to the obtained bone cement. In addition, bioactivity and biodegradation analyzes were performed by keeping the tissue scaffolds in artificial body fluid produced under laboratory conditions for various periods.

PART 2

LITERATURE REVIEW

Bioactive glass is both hemostatic and bacteriostatic and inhibits bacterial growth at the interface. This occurs when the high pH (up to pH 10) occurring on the surface of the glass inhibits bacterial growth and neutralizes the acids resulting from the infection [23]. It has been reported that almost no cellular reaction against the graft material occurs in cases where bioactive glass is applied and that bioactive glass minimizes the inflammatory response and macrophage activity [24].

Oonishi et al. [25] reported in their study that manipulating bioactive glass is easy and hemostatic effective. The most significant advantage of bioactive glass is its high surface reaction rate, which allows fast tissue bonding. Another advantage is that the elasticity coefficient values are close to the cortical bone. The feature distinguishing bioactive glass from other alloplastic materials is its ability to bind chemically to bony and soft tissues. Bioactive glass increases the proliferation of cells in new bone tissue [26].

While producing the material, it is aimed to increase the reactivity of the particles by reducing the size of the bioactive glass particles to nano levels. In this way, besides increasing the material's performance, new application areas are gained. Applying bioactive glass aims to provide faster ion release from the surface of the glass particles and, simultaneously, increase.

Bioactive glasses have many medical uses. It is primarily used in bone tissue repair and regeneration in bone defects, biomedical applications (middle ear surgery), clinical treatment of periodontal diseases, and coating of implant surfaces. It was determined that the resorption was completed in the following weeks. All of the tissue repaired with bioactive glass has transformed into bone tissue, and it has been reported.

that it does not consist of a mixture of material and bone as in other bone substitute materials [25], it has been determined that used bioactive glass for craniofacial reconstruction in 2 weeks and 12 weeks in cases when hydroxyapatite was applied. It has also been reported that the tissue formed when bioactive glass is used is trabecular bone.

A study comparing autogenous graft and bioactive glass on dogs found that the bone repair rate was higher in the bioactive glass. It is thought that the release of soluble silicon from the bioactive glass surface and activation of the stem cells of osteoblasts are thought to be effective in this. In a study by Elshahat et al. [27] in which they compared bioactive glass and calcium phosphate cement in cranioplasty, it was reported that while the bone cement remained unchanged and did not transform into bone tissue, bioactive glass activates bone formation and effortlessly merges with the cranial bone.

Amato et al. [28] reported that the bioactive glass they applied in enophthalmos is a biocompatible, easy-to-use material and stimulates bone growth. Some studies reported that bioactive glass can be safely applied as a coating material around titanium implants in rabbit tibia. , it was reported that bioactive glass was an excellent graft material in increasing bone healing [29].

A previous study has focused on lowering the melting point and improving the properties of bioactive glass-ceramic by adding various additives like Boron oxide.V2O5 is the other additive; it has the effect of improving the mechanical properties and speeding up the reaction of the sample when soaked in body fluid, and it promotes crystallization at relatively low temperatures above 600 0C. However, finding the eutectic point between two oxides and then adding or replacing it with glass components has not been the subject of any research.

M.R. Majhi et al. [30] used a conventional melting procedure in an electric furnace set to 1400 ^{o}C to create the bioactive glass 45S5 (Hench glass), with the composition 45 SiO_2 - 24.5 Na_2O - 24.5 CaO - 6 P_2O_5 (wt%). They also added Li_2O, K_2O, ZnO, MgO, and B_2O_3. K_2O's influence in place of Na2O in the bioactive glass 45S5 lowers glass transition and crystallization temperatures, while an increase in Li_2O and K_2O concentration in the bio-glass mixture improves density and compressive strength. According to FTIR absorption spectroscopy, the bioactive glass 45S5 loses some of its potency when B_2O_3 is substituted for SiO_2; the bioactivity barely shifts when Li_2O

and K_2O are used instead of Na_2O, and the bioactivity drops again when MgO and ZnO are substituted for CaO.

Deliormanli, A. M., et al [31]. $CaCO_3$, Na_2CO_3, $MgCO_3$, K_2CO_3, H_3BO_3, $CaHPO_4.2H_2O$, and V_2O_5(0.15,1,3)% were melted in the air and cooled between stainless steel plates after being heated to 1100 0C in a platinum crucible for an hour. Based on the data, vanadium-containing scaffolds deteriorated more quickly than their bare borate glass counterparts. The FTIR and SEM results showed that the vanadium-containing borate glass scaffolds and powders maintained their in vitro bioactivity even at high substitution levels. Twenty days of immersion in SBF resulted in a crystalline HA conversion layer on the 3% vanadium glass. Incorporating this ion resulted in a reduction in density, and the Vickers micro hardness of unmodified borate glass was greater than that of the substituted samples when subjected to high indentation loads. By forming triangular BO_3 groups, vanadium was found to presumably act as an intermediate ion and relax the borate glass network. Borate-based bioactive glasses containing V_2O_5 are promising materials with potential medical applications.

According to the composition of the glasses (24.5Na_2O, 24.5CaO, 6 P_2O_5-$xV_2O_5$and(45-xSiO_2) mol% (x =0, 3, 6, 9, 12&15 mole%), the batches were melted at 1250°C for 2 hours and cast into preheated stainless steel molds in 2016. At a sintering temperature of 660 0C, the latter changed into a white opaque glass with a crystalline structure at proportions(6 moles%). Low-V_2O_5 glass networks remained amorphous and transparent after heating, while glasses containing V_2O_5 have the advantage of being easily crystallized. Apatite (A), Wollastonite (W), and a Modified Vanadate Phase are all byproducts of the sintering process. The structure and morphology of sintered glasses diverge from those in their as-prepared form. Well-formed species formed in thermally treated glass are most easily recognized by their needle-like structure. As a crystallization agent in the glass network, Vanadium sped up the material's reaction when doused in bodily fluid [32].

PART 3

THEORETICAL BACKGROUND

3.1. BIOCERAMICS

Bioceramics are a special subset of all semi-crystalline or non-crystalline ceramic materials specifically designed to repair and reconstruct diseased or damaged parts of the body [33]. The first known bioceramic material in history is calcium sulfate in ancient literature from around 1000 B.C. Calcium sulfate was suggested to be useful in repairing broken bones around 300 BC, and in the late 19th century, it began to be used in vivo as a bone filler by orthopedic surgeons [33]. Until the discovery of 45S5 bioglass by Hench and co-workers in the early 1970s, calcium orthophosphates were considered ideal materials for bone substitutes because of their chemical and crystallographic similarity to the mineral phase of mammalian bone [34]. The applications of bioceramics in medicine are mainly related to repairing hard tissues such as bones and teeth. Over the years, dozens of compounds have been researched and clinically tested. Classifying bioceramics according to their bioinert, bioactive or bioresorbable properties depends on their interactions with tissues is possible. When ceramics, which can be considered almost inert, such as alumina and zirconia, are introduced into the body, they form filamentous tissue (fibrosis) at the interface. The clinical success of bioinert ceramics depends on their placement in the tissue with very good mechanical compatibility. This prevents mobility at the interface between implant and tissue (morphological fixation), making the fibrous tissue very thin. Otherwise, if they are placed in a way that allows mobility at the interface, the resulting fibrous tissue will thicken, and the implant will loosen.

Bioactive ceramics are ceramics where bonding occurs at the interface with living tissue or bone. This connection at the interface prevents mobility between the implant and tissue and also prevents the implant from being excluded from the body.

Since bioresorbable, i.e. biodegradable, ceramics are chemically degradable by body fluids,

when placed in the body after the repair process is complete, it dissolves and is destroyed by being absorbed by the surrounding tissue [35].

Table 3.1. Classification of bioceramic materials according to their interaction with tissue [4].

Implant type	Tissue response	Example
Non-porous, dense and inert ceramics	Very thin fibrous tissue formation (morphological fixation)	Alumina (Al), Zirconia(Zr)
Porous inert ceramics	Tissue growth within the pore (fixation)	Hydroxyapatite (HA)
Non-porous, bioactive ceramics	Tissue-implant interface bonding (bioactive fixation)	Bioactive glasses, Glass-ceramics, HA
Biodegradable ceramic	Absorption	bioactive glasses, Tricalcium phosphate

Due to their mechanical properties and composition, bioceramics are used for many different purposes. Bio-inert ceramics such as aluminum oxide, zirconium oxide and their composites are suitable for joint prostheses due to their excellent wear and friction properties. Bioactive glasses, particularly bioactive hydroxyapatite ceramics, which are not durable enough for orthopedic, load-bearing applications, are used to coat metallic biomaterials in direct contact with bone and support bone formation and regeneration. Apart from this, they are generally used for dental treatment and the treatment of middle ear bones. Bioactive glasses are considered suitable materials for producing scaffolds used in bone tissue engineering [36].

On the other hand, bioactive glass ceramics are preferred for treating more stressed areas such as the pelvis and spine. Apart from these applications, they are used in treating ear bones (hammer-anvil-stapes) and as bone-filling material in powder form.

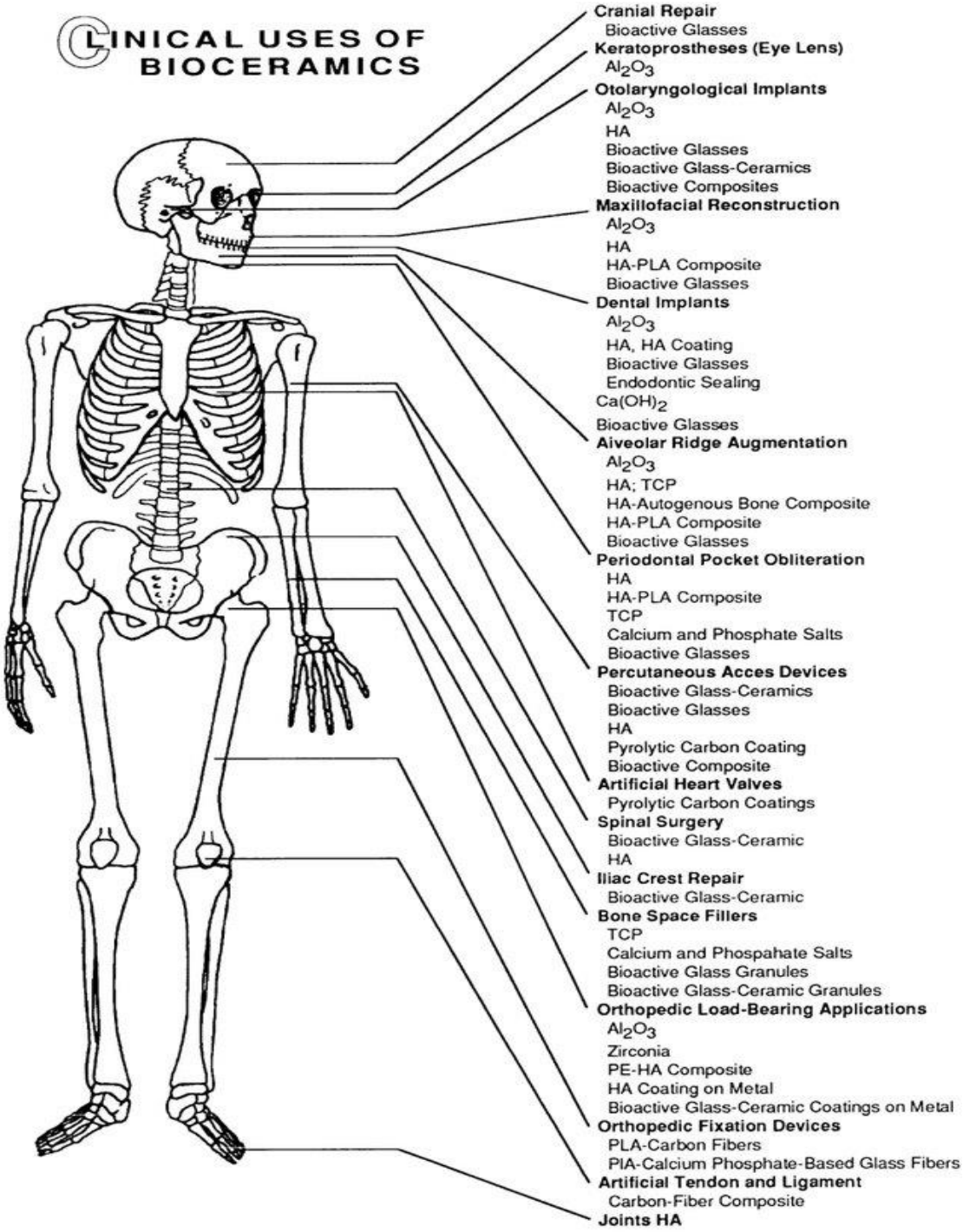

Figure 3.1. Usage Areas of Bioceramic Materials [37].

Bioactive materials are intended to produce a specific biological activity. Some specific bioactive materials form bonds with soft tissue. In many cases, however, the desired biological activity is for the bioactive materials to fuse with living body tissue and form a strong bond at the interface with the bone with which they are in

contact. Using an implant made of a suitable, bioactive solid material creates a fast and strong connection between the implant and the bone. Thus, implant materials are fixed without needing a mechanical fixation method (e.g. screws), bone cement (e.g. polymethyl methacrylate) or implant materials with a specially designed porous surface on which bone tissue can grow. The concept of bioactivity encompasses different bioactive materials belonging to various material classes with a wide range of bonding ratios and interfacial bonding layer thicknesses. Bioactive materials all form bonds at the bone interface; Bond time dependence, bond strength, bonding mechanism, bond area thickness, mechanical strength, and fracture toughness vary by material type. Recently, research has focused on developing bioactive ceramic materials for prostheses and implants. Research on bioactive glass ceramics, in particular, is attracting attention. Glass-ceramics are fine-grained polycrystalline materials produced by heat treatment and controlled crystallization of glasses of suitable composition. All bioactive implant materials have in common that they form a biological hydroxyapatite phase [hydroxycarbonate apatite (HCA)] on their surfaces during implantation [4]. Hydroxyapatite (HA, chemical formula $Ca_{10}(PO_4)_6(OH)_2$) is one of the most biocompatible materials because it is very similar to the mineral component of bones and teeth. HA-based materials show no toxic effects. It shows excellent biocompatibility with hard tissue and skin and muscle tissue. In addition, HA can bind directly to bone, and the stress gradient at the bioactive interface between implant and tissue is closer to that naturally occurring [38].

3.2. BIOACTIVE GLASSES

Bioactive glasses, a group of synthetic silicate-based ceramics first described by Hench et al., were developed. In 1969, specific proportions of silicon dioxide (SiO_2), sodium oxide (Na_2O), calcium oxide (CaO) and phosphorus pentoxide (P_2O_5) compounds were formed [48].]. The composition of this first-ever amorphous bioactive glass; consists of 45% by weight SiO_2, 24.5% by weight CaO, 24.5% by weight Na_2O and 6% by weight P_2O_5 and, due to its SiO_2 content of 45% by weight and the CaO /P_2O_5 ratio of 5 mol as 45S5 bioglass [4]. Subsequently, various bioactive glasses and glass-ceramics were obtained by adding components such as

potassium oxide (K_2O), magnesium oxide (MgO) and boron oxide (B_2O) to the structure of this composition. The compositions of various bioactive glasses and glass-ceramics developed from bioactive glass 45S5 are listed in Table 3.2.

Table 3.2. Components of bioactive glass and glass-ceramics (% wt.)[4].

	45S5 bioglass	**45S5F bioglass**	**45S5.4F bioglass**	**40S5B5 bioglass**	**52S4.6 bioglass**	**55S4.3 bioglass**	**KGC Ceravital**	**A-W GC**
SiO_2	45	45	45	40	52	55	46.2	34.2
P_2O_5	6	6	6	6	6	6		16.3
CaO	24.5	12.25	14.7	24.5	21	19.5	20.2	44.9
$Ca(PO_3)_2$							25.5	
CaF_2		12.25	9.8					0.5
MgO							2.9	4.6
Na_2O	24.5	24.5	24.5	24.5	21	19.5	4.8	
K_2O							0.4	
B_2O_3								
Form	Glass	Glass	Glass	Glass	Glass	Glass-ceramic	Glass-ceramic	Glass-ceramic

The critical component in the structure of bioactive glasses is silicate, accounting for 45-52% by weight. This silicate content is the essential feature that distinguishes bioactive glasses from conventional soda-lime-silica glasses. Another feature is that bioactive glasses have a high Na_2O and CaO content and a high CaO/P_2O_5 ratio. When bioglasses are exposed to body fluids, these properties result in a strong bond between host tissue or bone. This binding is believed to be due to the deposition of silicon ions and the formation of a hydroxyapatite coating on the surface of the bioglass [39]. The hydroxyapatite layer absorbs proteins and attracts osteoprogenitor cells (cells that secrete bone connective tissue), resulting in bone formation [4].

Therefore, the composition of bioactive glasses is essential for their ability to bind to living tissue. Therefore, Hench created a phase diagram describing the dependence of bone and soft tissue binding on the composition of Na_2O-CaO-P_2O_5-SiO_2 glasses.
The area where bioactive glass and glass-ceramic can bind to living tissue, such as bone, is indicated by the A region, and this area is referred to as the bioactive bone bonding limit. Zone B glasses have more than 60% silicate, such as window, bottle or microscope glasses. These glasses act like almost inert materials and expose fibrous tissue in the bone [4].

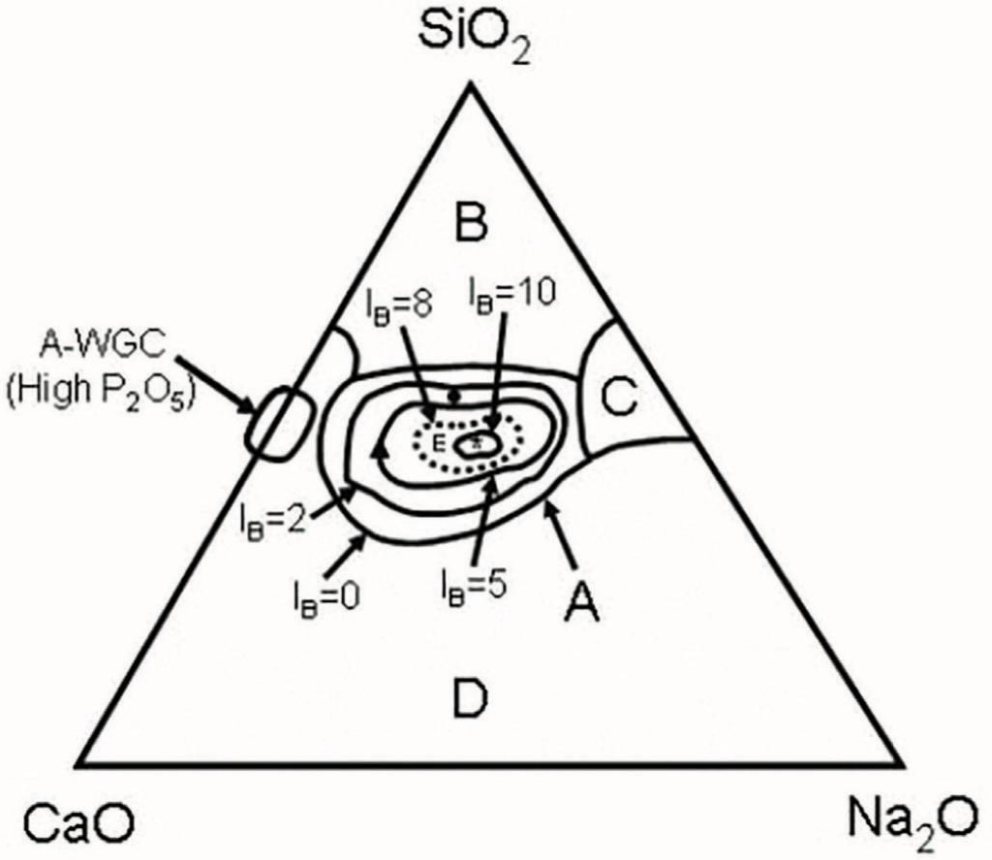

Figure 3.2. Phase diagram drawn by Hench; Compositional relevance of bioactive glasses and glass-ceramics to bone and soft tissue bond (% wt.). All compounds in zone A have a constant 6% P2O5. A-W glass-ceramic has a higher P2O5 content (see Table 3.1.). IB: Bioactivity index [40].

Glasses in the C zone are absorbable and disappear within 10 to 30 days after implantation. Spectacles in zone D are technically impractical and, therefore, not tested as implants. Glasses with the highest bioactivity and the fastest binding to bone tissue are in the E region in the middle of the diagram. As a result of the

studies, it was observed that glasses with a CaO/P_2O_5 ratio of less than 5 mol% show no bone adhesion. However, when B_2O_5 was added instead of silica in an amount of 5-15 wt% and CaF_2 instead of 12.5 wt% CaO, it was found that the bioactivity property persisted [40]. Furthermore, it was observed that adding 0–5% alkali to bioactive glasses did not prevent binding to bone but reduced bioactivity.

Bioactive glasses form a hydroxyapatite layer on all surfaces, not just in the contact area. This layer absorbs proteins and attracts osteoprogenitor cells (cells that secrete bone connective tissue), resulting in bone formation [41]. Furthermore, in cases where fractures occur during the application of bioactive glasses and if the parts are not separated, surface recombination can occur thanks to the self-repairing ability of the hydroxyapatite layer [35]. Another feature of bioactive glasses is that they have bacteriostatic properties. This is explained by the high pH (up to 10) formed on the surface of bioactive glasses reduces bacterial growth and neutralizes the acids formed due to infection. The most significant disadvantage of bioactive glasses is their amorphous structure and bidirectional glass network; however, they have low mechanical properties. The mechanical property values of various bioactive glasses and glass-ceramics are listed in Table 3.2.

Table 3.3. Mechanical properties of some bioactive glass and glass-ceramics [42].

Bioceramic	**Density (g/cm^3)**	**Compressive strength (MPa)**	**Tensile strength (MPa)**	**Modulus of Elasticity (GPa)**	**Fracture Toughness ($MPa.m^{-1/2}$)**
45S5	2.66	500	40-60	35	0.5-1
A/W glass ceramic	3.07	1080	215	118	2
HA	3.16	500-1000	115-200	80-110	1
Bioverit	2.8	500	100-160	70-88	0.5-1
Ceravital	-	500	-	100-150	-

As shown in Table 3.2, HA bioactive ceramics and A/W glass-ceramic bioactive materials have the highest compressive strength among the ceramic bioactive

materials. Although the values of the coefficient of elasticity of the 45S5 bioactive glass are close to those of cortical bone (see Table 3.3.), the tensile strength is between 40 and 60 MPa, which is considered insufficient in terms of its load-bearing capacity. Therefore, bioglasses are mostly used as coating materials [4].

3.3. MECHANISM OF BONDING OF BIOACTIVE GLASSES TO BONE

Hench et al. reported that bioactive glasses strongly bind to bone by forming a Ca-P-rich layer at the interface with bone. This bonding is achieved due to chemical reactions that start with surface dissolution and occur one after another on the surfaces of bioglasses when exposed to body fluid [43]. A series of 11 reaction steps occur on the surface of bioactive glasses, which are shown in Figure 3.3. economically viable. It is mainly present in igneous rocks, the sediments derived from them, and many silicates replacing silicon. Metallic titanium, in the state in which it is mined from ore, is called sponge titanium. This is due to its porous aspect that gives the appearance of a sponge. In the ore from which it is extracted, it is found to form rutile (TiO_2) or ilmenite ($FeTiO_3$)[44].

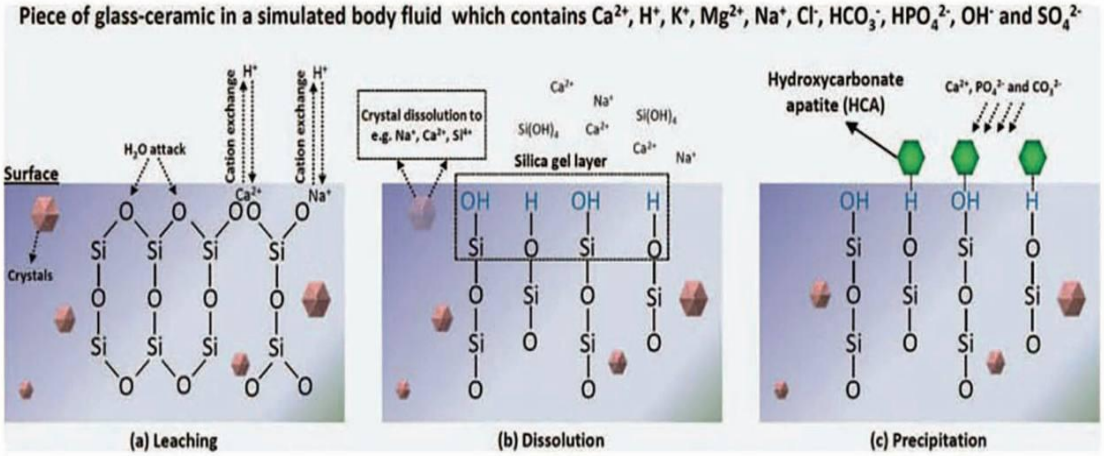

Figure 3.3. Reaction steps on the bioglass surface [45].

Stages 1 and 2 involve the dissolution of alkali ions in the structure of the glass and hydrogen ions in the solution to form Si-OH groups.

In step 3, with the polymerization reactions of the Si-OH groups formed, a 1-2 μm thick silica gel layer is formed on the surface [45].

Step 4, on the silica gel layer formed after polymerization, OH^-/ PO_4^{-3} ions in the solution combine with calcium ions (Ca^+) to form an amorphous calcium phosphate (CaO–P2O5) layer. The amount of Ca^{+2} and PO_4^{-3} in the solution effectively forms the calcium phosphate layer. The ratio of Ca+2 and Si(OH)4 is significant in hydroxyapatite formation.

In stage 5, the amorphous calcium phosphate layer combines with OH^-, $(CO_3)^{-2}$ ions from the solution, crystallizes and turns into a hydroxyapatite layer. For the hydroxyapatite layer to form, the Ca/P ratio should be 1.65 and above [46].

These first five stages of surface reactions occur rapidly and are completed within 24 hours for bioactive glasses in the E zone with the highest bioactivity, such as 45S5 Bioglass® [45].

Once the apatite core is formed on the surface, calcium and phosphate ions are removed, and growth continues spontaneously.

In stage 6, growth factors produced by cells increase adsorption and desorption. The time macrophages require to prepare the implant site for tissue repair and the attachment time is provided in stages 7 and 8, respectively. The 9th and 10 th stages affects the time of simultaneous proliferation and differentiation of osteoblast cells.

Finally, in the 11th step, the matrix's mineralization occurs, and the osteocyte cells are embedded in the collagen-HCA matrix. This whole process takes place within 6-12 days [4].

3.4. THE EFFECT OF BIOACTIVE GLASS ADDITIVES ON BIOLOGICAL PROPERTIES

Since the invention of 45S5 Bioglass, silicate-based bioactive glasses have been used in many applications in the biomedical field due to their ability to bond to bone [34]. Specifically, bioactive glasses form a layer of HCA on the surface when exposed to biological fluid, providing strong bonding to the bone. Recently, the effects of dissolving ionic products from bioactive glasses on osteogenic (bone formation) and angiogenic (new vessel formation) processes have been investigated. Studies have shown that ions are released from bioactive glasses; It has been shown that it

increases the proliferation of bone-forming cells, increases the production of insulin-like growth factor II, cell cycle regulators, and regulates protein production levels of numerous genes [47].

Bone tissue, which has the ability to regenerate itself, also contains blood vessels [48]. Various approaches, such as hormones and growth factors, have been proposed to promote bone formation and regeneration [49]. However, careless and misusing growth factors have caused some side effects, and safety has become an issue [50]. Alternatively, the incorporation or local delivery of bioinorganic ions, a natural but safer approach, has been emphasized [51]. Compared to growth factors, bioinorganic substances are receiving increasing attention due to their lower cost-effectiveness and more sustainable activity after application [52]. Some ions effective on bone formation and regeneration are shown in Table 3.4.

Table 3.4. Effects of some bioinorganic ions on bone formation

Ions	**Effect**
Mg^{+2}	Contributes to new bone formation. It increases the adhesion and stability of bone cells [53].
Sr^{+2}	Supports bone formation and development. It acts as a therapeutic agent in osteoporosis [54].
Si^{+2}	Triggers HCA formation in biological fluid environments. It ensures bone formation [55]. It increases bone density [56].
Zn^{+2}	A gene for differentiation of bone-forming cells. It regulates bone structure by increasing the protein synthesis of these cells. Contributes to its formation [57].
Cu^{+2}	Accelerates bone formation.

	It promotes blood vessel formation[58].
Li^{+2}	Stimulates the proliferation, differentiation and proliferation of bone tissue-forming cells.
	It supports bone formation by providing maturation [58].
Co^{+2}	Contributes to blood vessel formation and development [58]

3.4.1. Boron

Boron minerals contain variable proportions of boron oxide [B_2O_3]. Common boron minerals are tincal, colemanite, and ulexite [59]. Ulexite is the main boron mineral used in the manufacture of boron compounds. The chemical formula of ulexite is $Na_2O.2CaO.5B_2O_3.16H_2O$ with a complex structure and a sodium calcium borate type. The most commonly used boron compounds are boron oxide, boric acid and sodium perborate. Ulexite is one of the primary raw materials used to produce these compounds [60]. Colemanite's chemical formula is $2CaO.3B_2O_3.5H_2O$, the most common monoclinic crystalline boron mineral. Colemanite ore is used to produce boric acid [H_3BO_3] and fibreglass. Colemanite ore mainly contains clay minerals, strontium borate also contains other minerals such as calcite applications; glass, ceramics, nuclear, electrical, electronics and computer industries; Communications, building cement, metallurgy and energy sector, automotive industry, textile industry, chemical, cleaning and bleaching industry, agricultural sector, paper industry, photography, manufacture of composite materials and sports equipment, magnetic devices and mummification chemicals [61]. In addition, there are uses for boron in the pharmaceutical and cosmetic industries (manufacture of disinfectants, antiseptics and toothpaste) and medicine. Multiple myeloma occurs in the diagnosis of intracranial tumours in osteoporosis, allergic diseases, psychiatric disorders, the treatment of arthritis and menopause, and in the treatment, diagnosis, and treatment of infectious diseases. In researching the antimicrobial properties of boron, the first boron-containing biomolecule is a type of antibiotic called boromycin, which is active against Streptomyces. Boromycin is active against Gram positive bacteria,

some fungi and protozoa but not against Gram nagative bacteria. Boric acid ester is comparable to clinically used antibiotics; Erythromycin, gentamicin and streptomycin have been reported [62]. Boron is attracting the attention of periodontal researchers with its antibacterial properties and known effects on the bone immune response. The antibacterial and anti-inflammatory effects of the boric acid compound have been reported in general medicine.

Boric acid esters have been shown to inhibit the enzyme of microorganisms as well as DNA methyltransferase and men-choking methyltransferase in Gram bacteria; HIV-1 protease, glycohydrolase and NAD formations from ADP-ribosyltransferase in Gram bacteria are the essential examples [62]. Boric acid is recommended to treat bacterial infections and local alternative antimicrobial agents. Boric acid is also effective in controlling various staph bacteria [63]. Because of their porous and hydrophilic nature, natural fibres such as cotton are more resistant to problems from microorganisms than synthetic fibres. On the other hand, the human body provides warmth, moisture and nutrients to the bacteria in the clothes that come into direct contact with it. This creates a perfect environment and favourable conditions for bacterial growth. The applications in the field are also very old since the pests of microorganisms in textile products have been known for a long time. Inorganic salts, spices, and herbs used by the Egyptians to preserve the tissues surrounding corn are among the oldest practices.

Antimicrobials commonly used in the textile industry are triclosan, quaternary ammonium salts, polybiguanide, N-halamines, chitosan, and metal and metal oxides. Many antimicrobial materials have been developed for the textile industry in recent years. These materials have many differences in chemical structure, mechanisms of action, human and environmental impact, adhesion to the products they use, resistance to various external factors, prices, and interactions with microorganisms [64]. In developed societies, the need for antimicrobial materials suitable for humans and the environment is growing, which is one of the reasons for the development of composite technologies. This enabled the use of the natural mineral boron to be achieved. By incorporating these particles into the material's structure, producing materials with more durable antimicrobial activity becomes one of the more exciting research topics.

3.4.2. Vanadium Pent Oxide

V_2O_5 is classified as an intermediate or network former because its oxygen coordination number in a crystalline phase is five, higher than the coordination number of typical network formers, between three and four [65]. This is where most of the body's vanadium compounds are found. In addition, many vanadium compounds promote cell proliferation at low concentrations but promote growth at high concentrations. Adding vanadium oxides to drinking water has been shown to improve tendon and ligament repair, accelerate collagen deposition during skin wound healing, and increase wound strength [31].

Crystallization is simplified with glasses containing V_2O_5 since their high crystallinity can be achieved at a lower sintering temperature than with V_2O_5-free glasses. Sintered glasses (between 500 and 800 °C) are generally subject to helpful transformation processes within the glass matrix. Ceramics benefit greatly from vanadium oxide due to its increased thermal shock resistance, mechanical strength, chemical stability, and bioactivity [66]. Using vanadium complexes has been shown to reduce pathological blood sugar levels. Because of their insulin-like properties, they are often referred to as insulin mimetics, insulin mimetics, or insulin enhancers. Vanadium's ability to exchange ligands or chelators with its environment [67] is probably responsible for its antidiabetic effects. It has been shown that apatite's nucleation and growth kinetics are improved using a nucleating agent (V_2O_5) that reduces the surface energy between the crystal and glass phases.

Based on promising results from cancer studies in mice, vanadium oxide is used to treat the disease. It was discovered that V_2O_5-NPs (nanoparticles) possess anti-antigenic abilities by preventing the proliferation of endothelial cells [68].

3.5. BIOACTIVE GLASS PRODUCTION METHODS

Bioactive glasses can be produced by melting at high temperatures or by the sol-gel method.

3.5.1. Sol-gel Method

The name sol-gel, which is expressed briefly from the first syllables of the words solution-gelation, means solution-gelation. It is the most suitable process for surface-reactive ceramics, intended to be used in powder form [69]. It is also called the cold method because the production can occur at room temperature. Gel formation occurs due to hydrolysis and condensation reactions of homogeneous solutions obtained by mixing with water, acid or alcohol. This gel structure obtained is converted into a glass structure by applying heat treatment.

Bioactive glasses obtained by the sol-gel method have many advantages compared to bioactive glasses obtained by the melting method:

• A much more homogeneous bioactive glass structure can be obtained at much lower temperatures compared to the melting method,

• Controlling grain size, shape and surface area

• Higher purity bioactive glass structure can be produced,

• Lower energy consumption, less material loss through evaporation, and much less air pollution thanks to the ability to obtain products at low temperatures,

• Better bioactive glass products can be obtained due to the feature of gel structure,

• The application of the sol-gel method to glass structures consisting of many different compositions and the realization of phase separation and crystallization, and the production of compositions that cannot be produced by melting,

• It enables the production of fine-formed special products in the film structure. However, Its disadvantages are:

• High raw material cost,

• Undesirable shrinkage may occur during the process,

• Formation of more porous structure than it should be,

• Length of the process

• Difficulty keeping the solution constant viscosity during gel structure formation [70].

3.5.2. Melting Method

The most crucial difference between this method and the sol-gel method is that the process is carried out at high temperatures. In order to form the bioactive glass structure, the starting materials in powder form (such as SiO2, CaCO3, Na2CO3 and P2O5) are mixed and then melted at a temperature determined in the range of 1300-1500 ˚C and homogenized. The melting temperature depends on the percentage of components in the glass composition to be prepared. Compositions containing high SiO2 and CaO require high melting temperatures. In order to obtain a homogeneous bioactive glass structure, the process itself can be divided into stages [71]. The bioactive glass material, shaped by moulding after high heat treatment, is annealed at lower temperatures in the range of 500-600 ˚C, preventing the formation of micro-cracks that may occur during cooling.

Melting is a versatile method that allows the creation of a wide variety of glass compositions by simply adjusting the amount and percentage of raw materials used. In addition, the melt-derived route to producing bioactive glasses has several disadvantages. For example, high melting temperatures, contamination from the crucible material and subsequent grinding processes (possible contamination with abrasive residues) can make it difficult to produce high-quality glass-ceramics [72]. The steps of making glass according to the two methods are shown in Figure 3.4. This procedure offers many advantages, such as a simple change in glass chemistry, cheap raw material prices, fast processing times and a large production (amount) of glass [4].

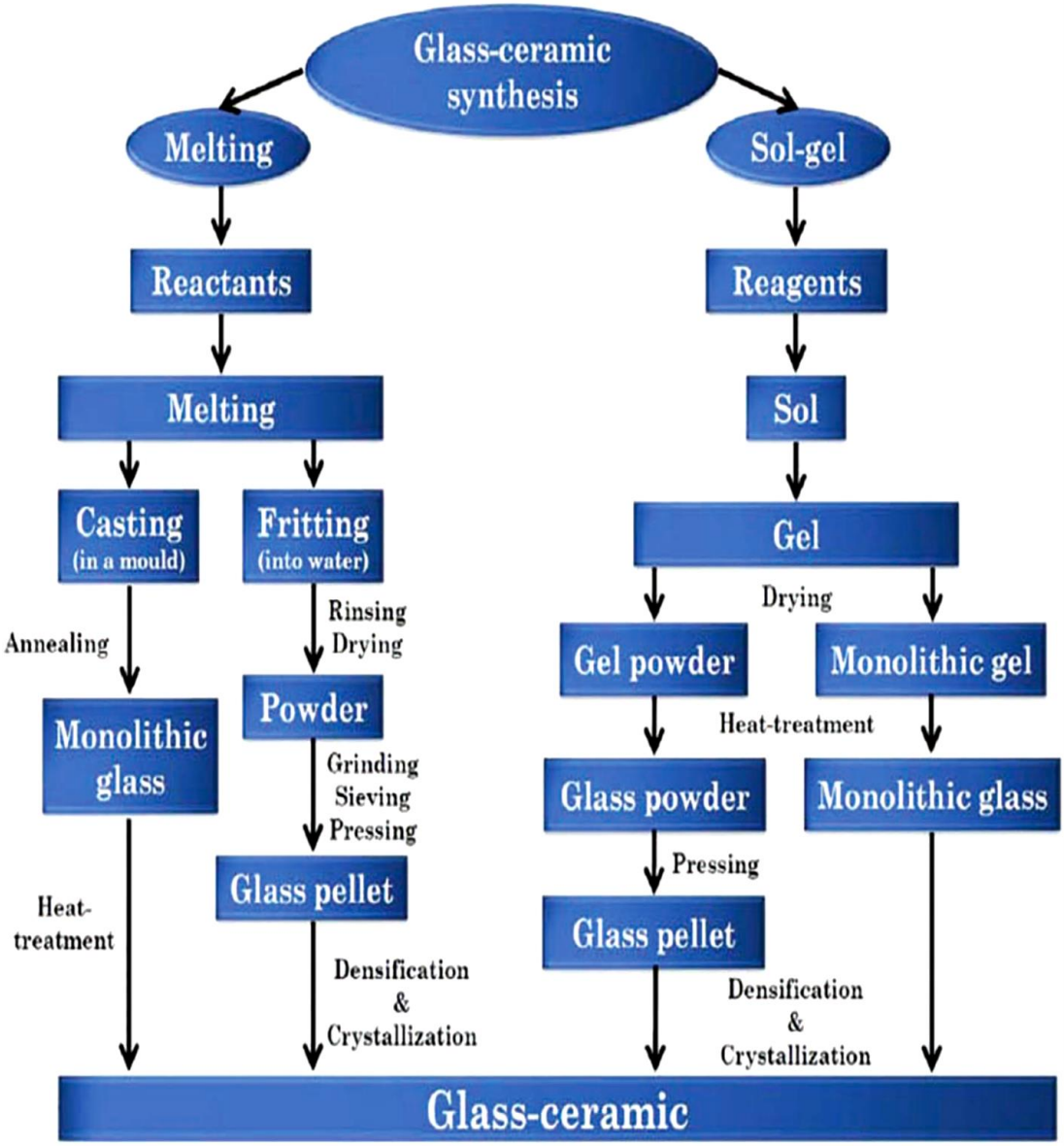

Figure 3.4. The main steps in the production of glass ceramics [4].

3.6. BONE CEMENT

Bone cement is one of the most commonly used products in orthopedics and traumatology. When it comes to bone cement, acrylic bone cement comes to mind. It has two main components, a liquid monomer and a powdered polymer. Alternative bone cement products emerge due to different combinations of substances with different properties in various proportions [73]. During the Second World War, when it was seen that some warplane pilots were injured by poly(methyl methacrylate) (PMMA) particles, and it was seen that PMMA did not cause any side effects or

chronic infections in the body as a result of these injuries, PMMA materials started to be used in the tissue as well. In this way, PMMA was developed in the 1940s by J. Judet and R. Judet at the articular head of the femoral bone.

It can be used to support the bone in the fixation of fractures in osteoporotic bones, and it is aimed to obtain a more solid fixation by strengthening the attachment of the screws used in the implant to the bone. Among the bone cement that can be used for filling purposes in the treatment of fractures, calcium phosphate-based bone cement comes to the fore [74]. Bone cement is divided into acrylic bone cement and calcium phosphate cement.

3.6.1. Calcium Phosphate Cement

Calcium phosphate cement is a bioactive substance. Calcium phosphate cement also contains powder and liquid components. Various calcium phosphate salts form the content of the powder part. Usually contains one or more of the following: Amorphous calcium phosphate (ACP), dicalcium phosphate dihydrate (DCPD), dicalcium phosphate anhydrous (DCPA), alpha-tricalcium phosphate (a-TCP), dicalcium phosphate (DCP), tricalcium phosphate (TTCP), monocalcium phosphate monohydrate (MCPM) or calcium carbonate (CC). The liquid component usually contains sodium phosphate and water. Calcium phosphate cement self-cures in the body similarly to acrylic bone cement. In this way, it can be applied while it is in dough consistency. They can even be injected into the area to be applied with appropriately sized injectors. Calcium phosphate cement is also known as hydraulic bone cement because water is the liquid required for their hardening. Their hardening occurs not due to polymerization like acrylic bone cement but because of dissolution and precipitation in water. Since this is not an exothermic reaction, it does not cause heat release [75]. Calcium phosphate cement is biocompatible, bioactive and osteoconductive because it can form direct bonds with bone. They are in the ceramic category as a biomaterial. Therefore, they are fragile. Since they have a porous structure, they are biomechanically weaker than acrylic bone cement. Despite the compressive strength of acrylic bone cement of about 2400 MPa, calcium phosphate cement only reach 25-50 MPa strength [76]. They can be used alone in non-loaded areas or combination with fixation materials (metal implant) in load-bearing areas.

Calcium phosphate cement has two end products, HAp or brushite (dicalcium phosphate dihydrate). Hydroxyapatite at pH>4.2 and brushite at pH<4.2 is the most stable calcium phosphate. Therefore, calcium phosphate cement containing apatite is common. Bruchite is physiologically found in acidic environments such as bone, fracture callus, and kidney stones. Therefore, brushite calcium phosphate cement absorbs faster than apatite calcium phosphate cement. The liquid/powder ratio of calcium phosphate cement; determines its plasticity, injectability and setting time. Even when exposed to blood or other body fluids, calcium phosphate cement freezes without losing its integral structure. The cohesion property of that material provides this. Calcium phosphate cement integrates better in the body thanks to its biological advantages, while at the same time, its subject to osteoclast resorption and remodelling. Since they are excreted from the body by cellular-based resorption, it is unlikely that a cavity will form again before new bone is formed due to rapid resorption at the place where they are placed [58].

Table 3.5. Comparison of Acrylic Bone Cement and Calcium Phosphate Cement [77, 78]

Feature	**Acrylic Bone Cement**	**Calcium phosphate cement**
Substance	Polymer	Ceramic
Liquid	Methyl Methacrylate	Water or liquid solutions
Powder	Polymethylmethacrylate	calcium phosphate powder
Hardening mechanism	polymerization	Dissolution and precipitation
Product	Polymethylmethacrylate	Calcium phosphate(HAp)
Exothermic Heat	50-90ºC	37ºC
Stability	Not resorbable	It will resorb
Bioactivity	Not bioactive	bioactive
Application	Moderately loaded areas, arthroplasty, vertebroplasty	Bone Regeneration, unloaded areas

3.6.2. Acrylic Bone

Cement Acrylic-based bone cement is widely used in orthopedics and dentistry to repair diseased or damaged parts of hard tissue and fix prostheses to the bone. Acrylic bone cement transfers the loads applied to the body from the implant to the bone and increases the load-bearing capacity of the implant-cement-bone system with the help of the mechanical bond it creates between the implant and the bone. Acrylic bone cement; consists of two parts, solid and liquid. Although their compositions vary, the solid part usually contains PMMA particles, polymer initiator, and various additives, and the liquid part contains methylmethacrylate (MMA) monomer and polymerization accelerator. Bone cement should not break during long-term use, the connection formed between the bone and the prosthesis should not loosen, and the heat generated during polymerization should not cause damage to the tissues. The most widely used acrylic is non-adhesive self-solidifying polymethylmethacrylate (PMMA). PMMA is a polymer commonly used in soft tissue injuries, joint infections, chronic osteomyelitis, and open bone fractures [79]. PMMA conforms to the shape of the environment in which it is found, allows many implants to spread, and is strongly bonded.

3.7. CLASSIFICATION OF BONE CEMENT

The length of the polymer chains, the molecular weight, the use of copolymer and the sterilization method can be counted among the factors determining cement's viscosity [77]. While gamma radiation shortens polymer chains, this is not seen in ethylene oxide sterilization. Sterilization with gamma or beta radiation lowers the molecular weight, which changes the mechanical properties of bone cement. Although ethylene oxide sterilization takes more time and is a more expensive process, ethylene oxide sterilization is the preferred method since it does not affect the molecular weight of the cement [80]. With the increase in viscosity after radical polymerization, some monomers cannot complete the polymerization. However, most of them gradually polymerize afterwards. The citric acid cycle metabolizes A small fraction into carbon dioxide and water. Bone cement is produced in three

different viscosities (viscosity); they can be examined in three sections as low, medium and high viscosity bone cement.

3.7.1. Low-Viscosity Bone Cement

The setting time is extended. During the working phase, the viscosity increases rapidly. The hardening phase is one or two minutes. Examples of low viscosity cement are Palacos“ LV (Heraeus), Palacios “ LV+G (Heraeus), Osteobond“ (Zimmer), Osteopal“ (Biomet Merck), Cemfix“ 3 (Teknimed), Sulcem“ 3 (Zimmer), C ~ment“ 3 (Fame), Genta C~ment“ 3 (Fame), Cemex“ RX (Exacttech), CMW“ 3 (DePuy), CMW“ 3 Gentamicin (DePuy) and Endurance“ (DePuy) can be counted[81].

3.7.2. Medium Viscosity Bone Cement

The setting time is long (approximately three minutes). During the working phase, the viscosity gradually increases. The hardening phase is around 1.5 to 2.5 minutes. Examples of medium viscosity cement are SimplexTM P (Stryker), SimplexTM P with Tobramycin (Stryker), SimplexTM P SpeedSet (Stryker), VersabondTM (Smith & Nephew), VersabondTM AB (Smith & Nephew), Smartset“ MV Endurance (DePuy), Smartset “GMV Endurance (DePuy), Palacios “ MV (Heraeus) (formerly Palamed“), Palacios “ MV+G (Heraeus) and Generation 4“ (Biomet) [82].

3.7.3. High-Viscosity Bone Cement

Adhesive setting time is short, and working time is extended, during which the cement is applied. Viscosity does not change until the end of the working phase. The hardening phase is around 1.5 to 2 minutes. Examples of high viscosity cement are Palacos“ R (Heraeus), Palacios “ R+G (Heraeus), Cemfix“ 1 (Teknimed), C~ment“ 1 (Fame), Genta C~ment“ 1 (Fame), Cemex“ ISO (Exacttech), Subiton“ (Prothoplast), Cobalt™ HV (Biomet), CobaltTM G-HV (Biomet), CMW“ 1 (DePuy), CMW“ 1 Gentamicin (DePuy) and SmartSet“ HV (DePuy) can be supplied [83]. The viscosities of bone cement mainly depend on its chemical structure and

polymer/monomer ratio. As the polymer/monomer ratio increases, the viscosity of the cement increases. Likewise, as the monomer/polymer ratio increases, the viscosity of the cement decreases and the hardening time increases. The only intervention that can be done to change the viscosity in operating room conditions is to cool the cement by keeping it at low temperatures before use. This is a method used especially in high-viscosity cement. Another factor that cement is sensitive to other than heat is humidity. Low temperature and high humidity prolong the setting time of the cement.

3.8. BONE CEMENT COMPONENTS

Acrylic bone cement has two main components: monomer in liquid form and polymer in powder form. Generally, the powder/liquid ratio is 2/1 [83]. The monomer methylmethacrylate (MMA) is the essential ingredient of the liquid part. It is a clear, colourless, pungent, flammable substance. Because the odor threshold is very low (0.2 ppm), the liquid monomer can be detected by its odor even in very small quantities. It has a boiling point of 100 °C and slightly irritates the skin. The liquid contains an activator other than the monomer. This is usually dimethyl-para-toluidine (DMpT). Although dimethyl-para-toluidine is known to be genotoxic, it is widely used, except that only one commercial cement contains an alternative amine, dimethyl-amino-phenyl-ethanol (DMAPE). Small amounts of hydroquinone are added to stabilize the liquid in order to extend its shelf life and prevent premature polymerization due to light or heat. Some liquids may contain chlorophyll to give it a green colour. The liquid components of bone cement on the market show similar properties [81]. We can see the content of the liquid and powder parts of bone cement and the purpose of their use in table 3.6.

Table 3.6 Components of Acrylic Bone Cement [84].

Acrylic Bone Cement			
Powder Components		**Liquid Components**	
Component	**Usage**	**Component**	**Usage**
Polymethylmethacrylate	Polymer	Methylmethacrylate, butylmethacrylate	Monomer
Methacrylate methylmethacrylate, Methyl Methacrylate Styrene	Copolymer	Dimethyl Paratoluidine	Activator
Barium sulfate, zirconium dioxide	Radiopacifier	Hydroquinone	Stability
Benzoyl peroxide			
Gentamicin,tobramycin, vancomycin	Antibiotic	Chlorophyll	color

3.8.1. PMMA

PMMA is a high-transparency thermoplastic polymer obtained by polymerization of methylmethacrylate monomer. Due to its transparency, aesthetics and scratch resistance, PMMA is a lightweight alternative to glass. Sometimes it is also called acrylic glass. PMMA can be an alternative to Polycarbonate (PC) if higher transparency, UV resistance and/or scratch resistance are required, and high-impact properties are not vital. PMMA was first produced by Rohm and Haas Company in 1933. PMMA is made possible as a thermoplastic pellet designed for injection, extrusion, and blow moulding. PMMA is an irregular polymer produced by the polymerization of methylmethacrylate [85]. In Figure 3.5, the polymerization of PMMA is shown with the chemical formula [86].

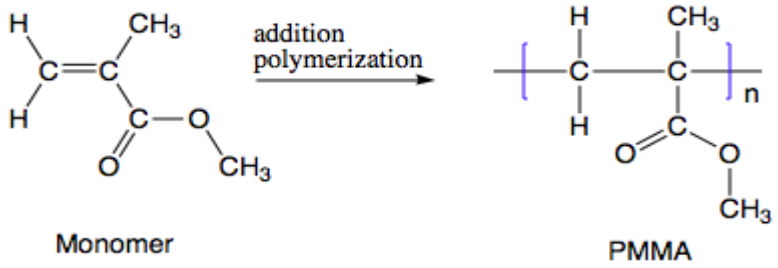

Figure 3.5. Demonstration of PMMA polymerization by chemical formula[86].

Exceptional optical properties, transparency and glossy appearance, rigidity and dimensional stability, hardness and scratch resistance, excellent resistance to sunlight (ultraviolet radiation) and weathering are among the main properties of PMMA[87]. PMMA can be formulated to achieve special properties and effects:

- Impact modification
- Food compatibility.
- Suitability for medical applications.
- UV transparency.
- Advanced chemical resistance.
- Resistance to gamma sterilization.

The abovementioned properties make PMMA the polymer of choice for the automotive, lighting, cosmetic and medical industries. Depending on the compositions, sizes and molecular weights, PMMA can be used in different applications :

- As an agent for thermoplastic blends,
- A thickening agent for bulk methylmethacrylate processes,
- Additive for some decorative coating systems.

Unlike other polymers, the mechanical properties of PMMA vary depending on temperature. Undoped PMMA is not high-strength resistant. In addition, it is one of the polymers that does not deteriorate when exposed to direct sunlight. UV rays make very small changes in PMMA structure in the presence of ozone. The tensile strength of PMMA is up to 70MPa. Its impact resistance is almost as high as HIPS. It is also an advantage that it is a plastic that can be processed in the machine. The bending temperature (HDT) of heat-resistant PMMA can reach over 90°C, and it is a

plastic that is generally easy to mold. Although it is resistant to many chemicals, it is not resistant to organic solvents. Polymethyl methacrylate; It is soluble with some solvents such as acetic acid, acetone, chloroform, trichloroethylene, benzene and toluene. Since the polymerization reaction is exothermic, it requires very good control [88].

3.8.2. MMA

The monomer methylmethacrylate (MMA) is the essential ingredient of the liquid part. It is a clear, colourless, pungent, flammable substance. Because the odour threshold is very low (0.2 ppm), the liquid monomer can be detected by its odor even in very small quantities. It has a boiling point of 100 °C and slightly irritates the skin [89].

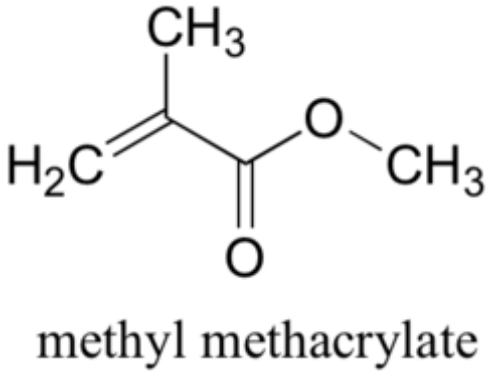

Figure 3.6. MMA chemical formula[90].

3.8.3. Benzoyl Peroxide

Benzoyl peroxide is used as an initiator to initiate the polymerization. Benzoyl peroxide is a suitable initiator, and when solutions prepared in solvents such as benzene and toluene are heated at 70–80 ºC, benzoyl oxy radical is produced by decomposing with the following reaction.

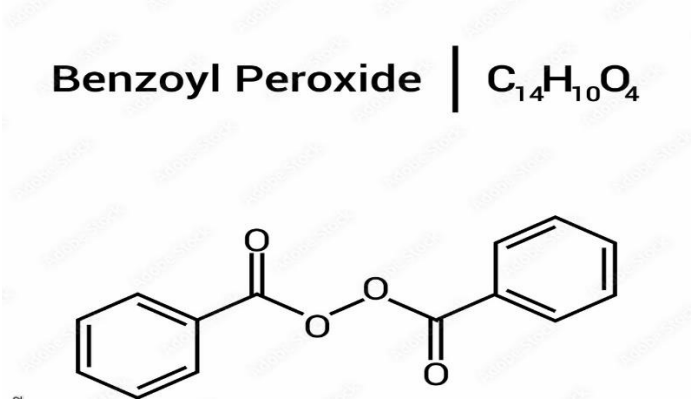

Figure 3.7 Benzoyl peroxide [91].

When a vinyl monomer such as acrylonitrile is present, the benzoyl oxy radical combines with the monomer over one of the π-electrons of the monomer to form the first monomeric radical. A new monomer is attached to the active center in the radical in the same way, and the radical active chain grows this way.

3.8.4. Radiopacifier

The use of cement in bones necessitates using radioopaque materials in terms of traceability, radiopaque substances used in commercially suitable cement are zirconium dioxide ZrO_2 and barium sulfate $BaSO_4$.

3.8.5. Accelerator

Dimethyl para toluidine; It is a material in the liquid part of bone cement as a chemical accelerator. The molecular structure of DMPT, whose chemical formula is $C_9H_{13}N$, is shown below.

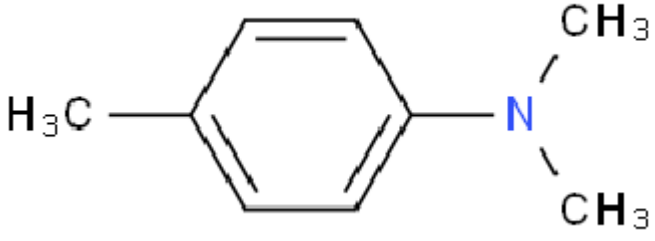

Figure 3.8. Molecular structure of 14 DMPT [92].

The monomer can begin to polymerize spontaneously by means of heat, light and oxygen. For this reason, inhibitors that prevent polymerization and prolong the storage time of the liquid are placed in the liquid part of the bone cement. Inhibitors slow down or stop a chemical reaction, while stabilizers act as stabilizers. Hydroquinone is usually added at a rate of 0.003% - 0.1% as an inhibitor [93]. The molecular structure and appearance of hydroquinone were as follows.

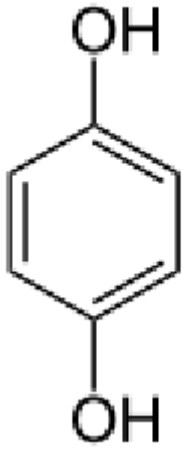

Figure 3.9 Molecular structure of 15 hydroquinone [93].

The biggest problem of bone cement to date is the decrease in mechanical strength due to various reasons and the occurrence of fractures. Many studies have been carried out to increase the mechanical strength of bone cement, and various additives have been used.

3.9. BIOCERAMIC ADDED BONE

Cement Hydroxyapatite is the principal mineral of bone and tooth. Chemical formula; It is in the form of $Ca_{10}(PO_4)_6(OH)_2$. Hydroxyapatite can be extracted from natural sources. Bovine bones and corals (through hydrothermal conversion) are examples of these natural resources. Hydroxyapatite can also be prepared artificially. Dağlılar and Erkan [94] compared the mechanical strength of bone cement reinforced

with hydroxyapatite, bovine hydroxyapatite and β-tricalcium phosphate treated with different amounts of silane. For this purpose, compressive strength, elastic modulus and 3-point bending strength measurements were made. Observations of the microstructure of the fracture/cracked surfaces were carried out with the help of SEM. While preparing bone cement, firstly, polymethylmethacrylate prepolymerization powders (mean particle size 40 μm) and methylmethacrylate liquid were used to prepare bovine hydroxyapatite powders, synthetic hydroxyapatite and β-tricalcium phosphate powders. Silane was added for the preparation of bioceramic-added bone cement. Commercially available bone cement CMW(TM) 3 was chosen as the reference. The results of the compression strength test performed according to the standards showed that the bone cement was strengthened when bioceramics were added. The strengthening effect is more pronounced in bovine hydroxyapatite than in hydroxyapatite and β-tricalcium phosphate. In previous studies, it was stated that the addition of a high amount of hydroxyapatite reduces compressive strength. The benefits of adding a small amount of bioceramics into bone cement are also evident from the flexural strength results. In these studies, it was also observed that the increase in hydroxyapatite caused a decrease in the compressive strength of the bone cement.

Bioactive glass is osteoconductive; wherever it is on the surface, when it comes into contact with a bone-forming cell, bone is formed there. Bone formation is seen on the entire surface of the bioactive glass, not just where it comes into contact with the bone. The bone-bonding feature of bioactive glasses is due to their high reactivity. As a result, the calcium phosphate layer is attached to the surface of the glass instead of the broken silicon bonds and then turns into hydroxycarbonate apatite (HCA) crystals [95]. Thanks to this feature, bioactive glasses can be chemically bonded to the surrounding hard tissue and, in some cases, to the soft tissue. The coating of the graft particles with the HCA layer occurs within a few hours after transplantation. This calcium phosphate-rich layer increases the adsorption and density of proteins used by osteoblasts to form a mineralized extracellular matrix [17].

It is thought that the positive contribution of bioactive glasses to bone formation in cell culture studies and in vivo applications is due to the formation of hydroxyapatite

and the formation of bone-implant connections, as well as the increase in collagen synthesis and cross-linking rate. Bioactive glass is both hemostatic and bacteriostatic and inhibits bacterial growth at the interface. This occurs when the high pH (up to pH 10) occurring on the surface of the glass inhibits bacterial growth and neutralizes the acids resulting from the infection.

Bioactive glasses have many medical uses. It is primarily used in bone tissue repair and regeneration in bone defects, biomedical applications (middle ear surgery), clinical treatment of periodontal diseases, and coating of implant surfaces [96]. The most significant advantage of bioactive glass is its high surface reaction rate, which allows fast tissue bonding. Another advantage is that the elasticity coefficient values are close to the cortical bone. The feature distinguishing bioactive glass from other alloplastic materials is its ability to bind chemically to bony and soft tissues. Bioactive glass particles accelerate new bone tissue proliferation[26]. While producing the material, it is aimed to increase the reactivity of the particles by reducing the size of the bioactive glass particles to nano levels. In this way, besides increasing the material's performance, new application areas are gained for the material. Applying bioactive glass aims to increase the bioactivity by performing both faster ion release and high protein adsorption from the surface of the glass particles. Grafts containing bioactive glass, which have been introduced in recent years, have shown that they can provide more new attachment and bone filling compared to other alloplasts [18].

PART 4

METHODOLOGY AND EXPERIMENT

4.1. INTRODUCTION

This chapter deals with the procedures of preparing bioactive glass-ceramic powders and bone cement. Moreover, it details the precursors and chemicals used, processing conditions and the characterization techniques employed during the experimental work.

4.2. PROGRAM OF THE PRESENT STUDY

Regardless of the compound to be synthesized and the details of the experiment, a general procedure was used throughout the current study to prepare bioactive glass. Figure 4.1 shows the steps which were followed in the general preparation procedure. Table 4.1 Prepared samples in the present study.

Table 4.1 Details of the chemical composition (in wt.%) of the glasses

Sample	The weight percentage of the element (wt.%)					
	SiO_2	Na_2Co_3	CaO	P_2O_5	B_2O_3	V_2O_5
SCNBV1	39.0	14.5	24.5	6.0	15.0	1.0
SCNBV3	37.0	14.5	24.5	6.0	15.0	3.0
SCNBV5	35.0	14.5	24.5	6.0	15.0	5.0

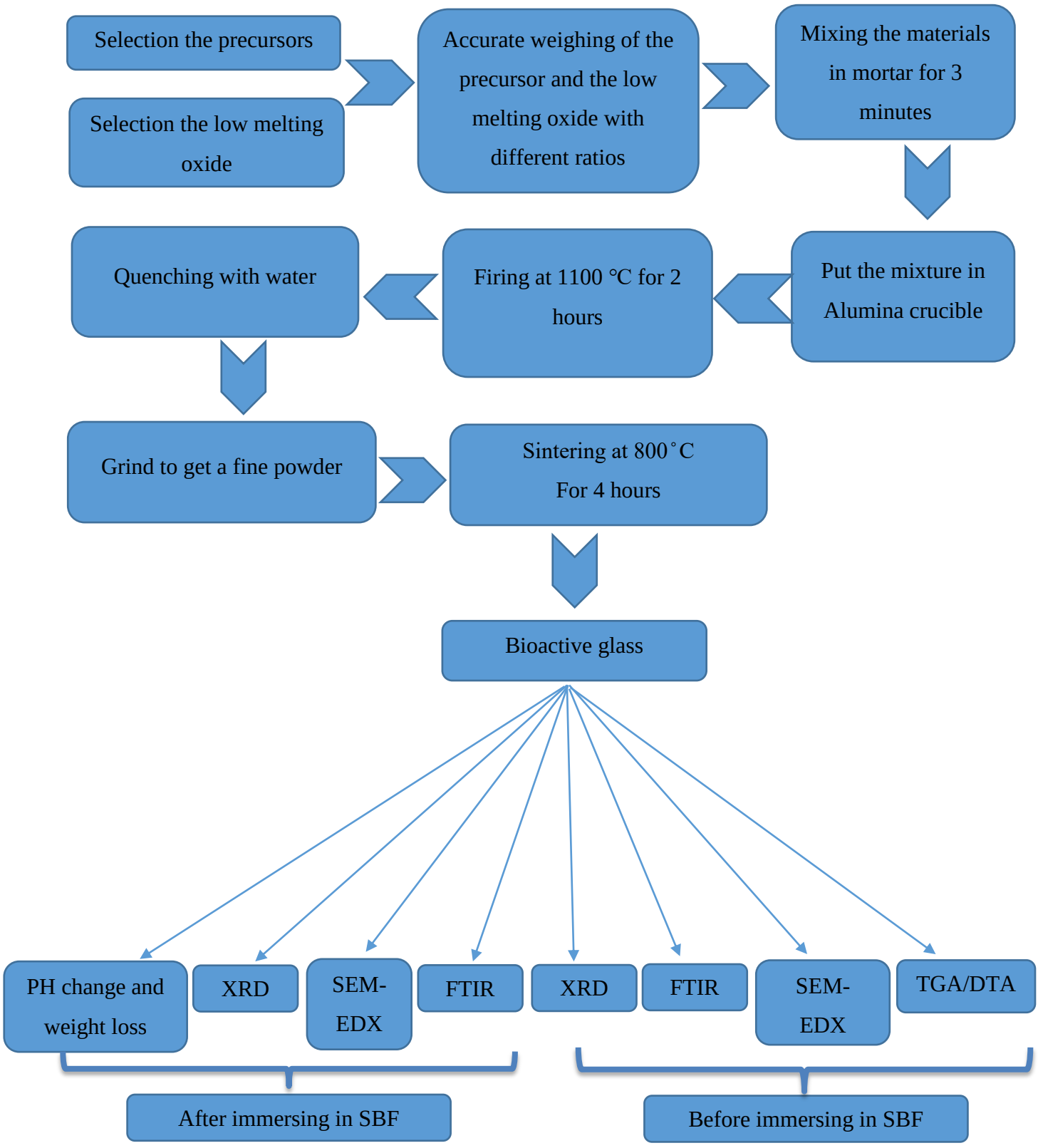

Figure 4.1 Flowchart of the general preparation procedure used in the current study

4.3. PREPARATION OF BIOACTIVE GLASS-CERAMIC POWDER

The modified 45S5 bioglass ceramic analogues were SiO_2, CaO, NaO, P_2O_5, B_2O_3, and V_2O_5. The various chemical compositions of the bioactive glass ceramics obtained are presented in Table 4.1. To be more specific, varying concentrations of V_2O_5 were added by employing a melt-quenching technique. Therefore, to facilitate easier abbreviation, the Na_2O-, CaO-, SiO_2, and B_2O_3-based bioglass ceramic with various V_2O_5(X) additions defined as NCSB(X)V (where X = 1, 3, and 5 wt. %). After thoroughly combining the oxides and the V_2O_5, the mixture was melted in an electric furnace using a platinum crucible at 1100 ℃ for 2 hours at a heating rate of 5℃/min (Figure 4.2). After removing the molten from the furnace, it was placed in a container with distilled water at room temperature. The powders were then milled after being placed in the container and sintered for four hours at an internal temperature of 800 ° C. The samples were allowed to cool in the furnace until they reached room temperature.

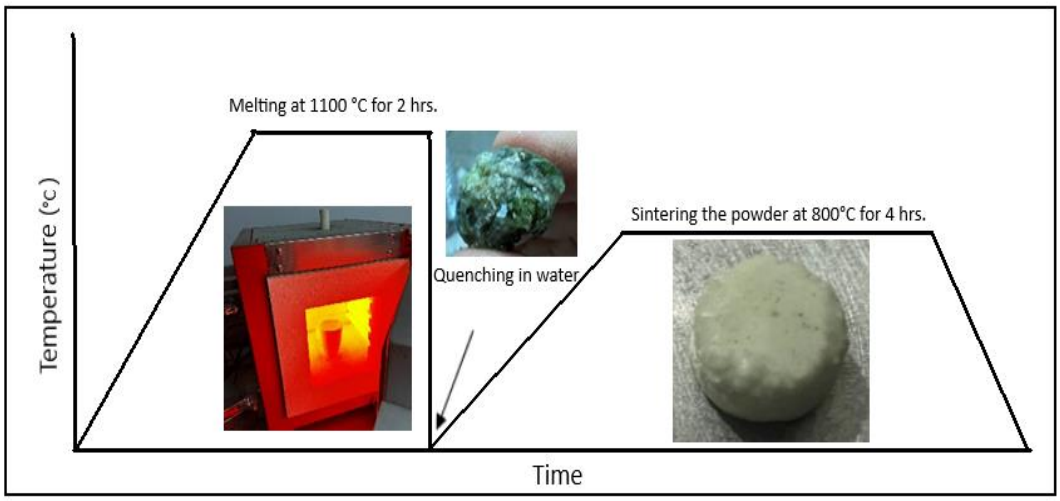

Figure 4.2. The procedure of bioactive glass-ceramic production.

Samples with a diameter of 6 mm and a length of 6 mm were produced in the mold under a pressure of 5 MPa. To make the 1.5% v/v solution of polyvinyl alcohol (PVA) (6 kDa), the temperature was set to 60 °C, and magnetic stirring was used. BG powders were mixed with the PVA solution, the binder's material. The mass ratio of the solution to the powder was 0.6:1. Utilizing a binder increases the powder's

plasticity, decreasing the possibility of crack formation due to pressing. And then, it was placed in a drying oven for 24 hours at a temperature of 60 °C. Finally, the green compacts were heated to 800 °C in an electric furnace (Ref-San (RD 16), Turkey) for 4 hours (holding time: 3 °C/min, heating rate: 3 °C/min), and then the furnace was allowed to cool down on its own (Figure 4.2).

4.4. CHARACTERIZATION

4.4.1. Differential thermal analysis (DTA)

DTA HITACHI-STA 7300 Model was used to determine the produced bioactive glass samples' glass transition temperatures (Tg) and crystallization temperatures (Tc). Tests were done at (IRON AND STEEL INSTITUTE / karabuk university). During a TG/DTA analysis, 19.78 mg of glass powder was heated from room temperature to 1000 °C at 10 °C/min.

4.4.2. X-ray Diffraction (XRD)

X-ray diffraction analysis (XRD) was performed using a RIGAKU XRD D/MAX/2200/PC device to determine the post-casting structures of bioactive glass samples to detect the crystal phases formed on the surface of both glasses as a result of bioactivity tests. CuKα beam with wavelength l=1.54056 is used, scanning angle (2θ) is between 10-60º and scanning speed is 2º/min. By examining the diffraction diagrams obtained, it was determined which phases were formed in bioactive glasses and tissue scaffolds after casting and soaking in artificial body fluid, after which a comparison was made with the various standard charts.

4.4.3. Fourier transform infrared Spectrometer (FTIR)

Infrared (FTIR) spectra of samples were recorded using (Shimadzu 1800, Japan) to evaluate the molecular structure of functional groups in inorganic materials. Tests were done at (IRON AND STEEL INSTITUTE / karabuk university). The FTIR study has been carried out to characterize the bioactive glass powders and bulk

samples after immersing them in SBF. The FTIR spectra were recorded on an infrared spectrophotometer with KBr pellets in the range 600 - 2500 cm^{-1} with (KBr: sample weight ratio of 100:1). Tests were carried out at room temperature.

4.4.4. Scanning Electron Microscope (SEM)

SEM and EDS analysis; scanning electron microscopy (SEM) ((Carl Zeiss ultra plus Gemini FESEM) and energy dispersive X-ray spectroscopy (EDS) (IXRF Instruments, IXRF, Inc, USA) (Figure 4.3). The specimen is imaged through a high-pack of electrons; this test was done at the University of Karabuk –Turkey. Randomly selected samples from each group were placed in the incubator, dried, and coated with Au-Pt with a spray coater. SEM images were obtained at 20kV acceleration voltage using the 12 mm working distance of the samples. The mineralization process was terminated using acetone; the samples were washed twice with ethanol and twice with deionized water; and lastly, the samples were dried in an oven set to 70 °C for 24 hrs. After that, scanning electron microscopy (SEM) was used to examine the morphology of the newly generated HCA on the sample's surface.

Figure 4.3 Scanning Electron Microscopy.

4.4.5. Weight Loss and PH analysis

Kokubo and his team developed a simulated liquid that almost equals ion concentrations in human blood plasma [97]. This liquid is also known as artificial body fluid (ABF) or Kokubo solution. The ion concentrations of human plasma by ABF are shown in Table 4.2.

Table 4.2. Ion Concentrations of the SBF and Human Blood Plasma [72].

Ion	**Concentration (mM)**	
	Simulated body fluid (SBF)	Human blood plasma
Na^+	142.0	142.0
K^+	5.0	5.0
Mg^{2+}	1.5	1.5
Ca^{2+}	2.5	2.5
Cl^-	147.8	103.0
HCO_3^-	4.2	27.0
HPO_4^{2-}	1.0	1.0
SO_4^2	0.5	0.5

The chemicals in Table 4.3 were used in the specified amounts to prepare artificial body fluid. 750 mL of pure water taken into a beaker is placed on a magnetic stirrer, the temperature at 36.5 °C. The chemicals specified in the table are added to the pure water in the order in which they are added. The solution pH does not change rapidly (CH2OH)3CNH2 chemical should be added slowly. In the last case, the pH of the solution is adjusted to 7.4 with 1 M HCl. Finally, the solution volume is completed to 1000 ml with distilled water at 36.5 °C.

Table 4.3. Chemical composition of simulated body fluid (SBF)[72, 97].

Reagent	Amount
NaCl (g)	8.036
$NaHCO_3$(g)	0.352
KCl(g)	0.225
$K_2HPO_4.3H_2O$(g)	0.230
$MgCl_2.6H_2O$(g)	0.311
1 M HCl (mL)	40
$CaCl_2$(g)	0.293
Na_2SO_4(g)	0.072
Tris (hydroxymethyl) aminomethane(g)	6.063

The analysis of the pH of the bioactive glass was carried out using an Akso® digital pH meter with a replaceable electrode. The equipment calibration was performed based on triplicate measurements of simulated body fluid solution (SBF), which has a pH of approximately 7.4. To measure the samples' pH, 0.20g of each cement was used for 20 mL of deionized water after the products had been in contact with the water at 37 °C for 2-21 days.

The procedure presented in the ISO 6876-2012 standard was adopted to evaluate weight loss. The samples of each cement were produced in the form of discs (10x6 mm). The bioactive glass specimens were placed in cylindrical plastic containers containing 20 mL of simulated body fluid (SBF) with ionic concentrations similar to human blood plasma. The containers were kept at room temperature for 2-21 days. After this period, they were removed from the liquid, dried in an oven at 37 degrees and analyzed. The solubility, according to the standard mentioned earlier, is defined as the difference between the initial mass (Mi) and the final mass (Mf) of a given specimen,

The weight reduction was computed as the equation:[72]

where $W = W_0 - Wt$,

W0 is the glass-ceramic starting mass, and Wt is the mass at time t. Three glass-ceramic of each material were used to quantify weight loss at each time point.

4.5. PREPARATION OF BONE CEMENT

The chemicals used in this study and the companies from which these were purchased are given in Table 2.1. All chemicals except methyl methacrylate (MMA) were used as received. MMA contains hydroquinone as an inhibitor to prevent premature polymerization.

Bone cement is a two-component and is prepared by mixing the solid and liquid parts. First, the materials to be used in the solid part were weighed and mixed homogeneously in a poly(propylene) container. The liquid portion was also prepared and stored in a glass bottle until used. Before the experiments, all materials were kept at room temperature for at least 1 hour. To prepare the bone cement paste, the liquid part was added to the solid part and mixed for 2-3 minutes until a homogeneous paste was obtained with the help of a spatula. All doughs were prepared in this way by mixing them by hand.

For bone cement, the powder part consisting of PMMA, Zirconium dioxide and Hydrous benzoyl was prepared homogeneously and then mixed with the liquid part consisting of MMA and N, N-dimethyl-p-toluidine (DMPT). Different compositions were prepared by adding various amounts of glass ceramics, as shown in Table 4.4. Since 2 mL of MMA was insufficient to wet the polymeric microspheres in the bone cement prepared in the third group, the ratio was changed, and 6 mL of MMA was used. In order to examine the effects of additives, different amounts of bioactive glass were added to the solid part, and dodecyl mercaptan was used as a chain stopper to the liquid part. In addition, the material compatibility between bioactive glass and PMMA was tried to be increased. To increase biocompatibility, 0%, 10% and 20 wt.% bioactive glass was added to the solid fraction. There is a certain critical ratio for bioactive glass added to the medium. In cases where the bioactive glass addition is less or more than this critical ratio, the mechanical strength is adversely affected. Adding bioactive glass above a specific rate disrupts the homogeneity of the bone cement paste and complicates the processing properties. Therefore, the optimum amount of bioactive glass was determined by trying different amounts. The

aim is that the active functional groups that will form on the surface form stronger chemical bonds in the bone cement structure and increase mechanical strength. This process positively affects the material compatibility between bioactive glass and PMMA and prevents the components from remaining in two separate phases by providing a homogeneous mixture.

Table 4.4. Mixing compositions of bone cement

Sample	**Filler loading (wt.%)**	**Powder parts**		**Liquids parts (ml)**	**Liquid-to-powder ratio(%)**
		PMMA(g)	Filler (g)		
Control	0	40	-	20	0.5
BCGC10	10	40	4	20	0.45
BCGC20	20	40	8	20	0.41

4.6. CHARACTERIZATION OF BONE CEMENT

In vitro and the mechanical properties of the prepared bone cement were investigated by tensile and compression tests. Mechanical experiments were performed at room temperature with the LLoyd LRX 5K (LLoyd Instruments Limited, Fareham, Hampshire, UK) mechanical measuring instrument.

4.6.1. In Vitro Studies

In order to increase the ion concentration, facilitate the formation of apatite cores and make the coating more efficient, a 1.5xSBF solution was prepared using the chemicals in Table 4.2.

In order to observe the formation of the hydroxyapatite layer on the surfaces of the produced samples, the samples were kept in 20 ml artificial body fluid for 7 days. During the waiting periods, the SBF solutions containing the samples were placed in the oven, and the temperature was kept constant at 37°C.

XRD analysis was applied to the samples to determine the crystal phases formed in the samples kept in SBF. The microstructures of the samples were determined using

SEM. All these analyzes were also applied to the samples that were not kept in SBF in order to be able to compare and examine the changes.

4.6.2. Tensile Tests

The bone cement paste was rolled out on a poly(ethylene) surface with the help of a roller. While the dough was still soft, tensile test specimens were prepared by cutting with a dog bone-shaped mold. After the dough was kept at room temperature for 1 hour to harden, it was kept in physiological saline for 24 hours at 37±1°Cto simulate the body environment. The prepared tensile specimens were pulled at a 1 mm/min speed in the LLoyd LRX 5K mechanical measuring device, and the elastic modulus (E) and tensile force (UTS) were calculated. For each sample, at least five samples were tested and averaged. The tensile test specimen and the test setup are shown in Figure 4.4.

Figure 4.4 Prepared tensile test specimen and tensile test setup.

4.6.3. Compression Test

A stainless steel compression mold conforming to ASTM F451-95 standard prepared the compression samples. The compression test specimen and test setup are shown in Figure 4.5. The mold consists of three cylindrical plates with a diameter of 84 mm and a height of 12 mm. The central plate has 52 holes, each 6 mm in diameter. While

the prepared dough was still soft, it was placed in this mold and compressed with the help of a vice. Elastic modulus (E) and compression force (UCS) were calculated by pressing the prepared compression samples at 25 mm/min speed on the LLoyd LRX 5K mechanical measuring device. At least eight samples were tested and averaged for each sample.

Figure 4.5. Compression mold and test setup

4.6.4. Setting time of Bone Cement

Thermal measurements were performed by placing a J-type thermocouple wire in the center of the spherical bone cement (approximately 15 mm in diameter). The temperature increase due to the heat generated during the polymerization was transferred to the computer using the \"SuperLogics 8018 Thermocouple Input Module\" and a temperature-time diagram was created. The experimental setup is shown in Figure 4.6. The curing time and the maximum curing temperature reached were determined from these diagrams. Temperature experiments were performed at room temperature, averaging 232 °C. The maximum curing temperature is the highest temperature reached during polymerization. The curing time is defined as the time when the temperature rise reaches the midpoint between the maximum temperature and the ambient temperature [98]. The curing temperature was calculated using the following formula.

A typical temperature-time graph showing the exothermic temperature change

observed as the bone cement hardens is given in Figure 4.8.

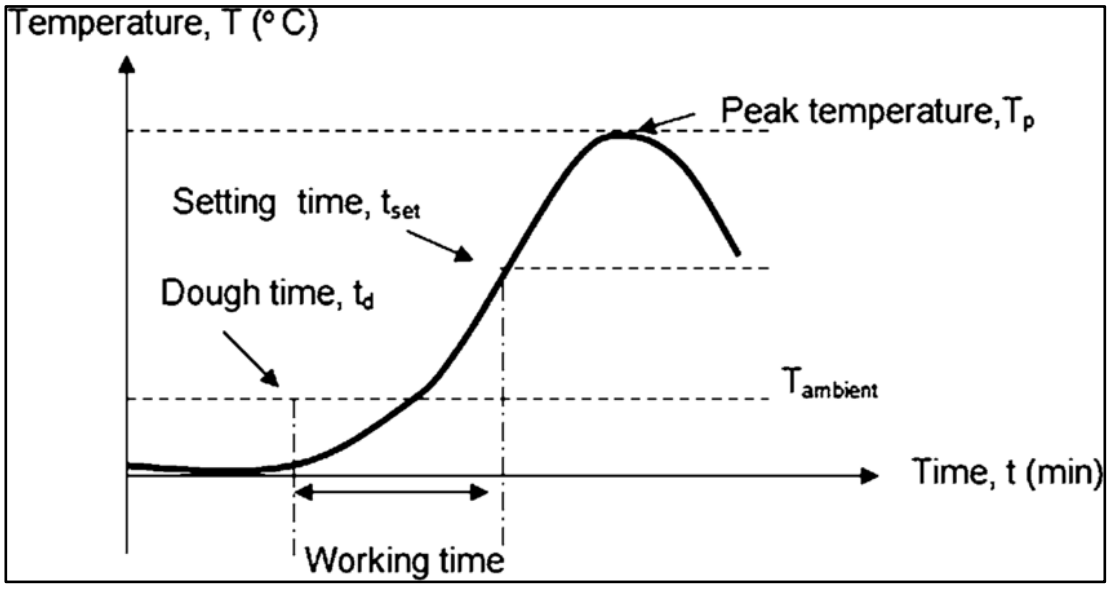

Figure 4.6. Temperature-time graph [99].

PART 5

RESULTS AND DISCUSSION

In orthopedic applications, especially prosthetic implants, PMMA-based bone cement is generally used as a retainer between the metal prosthesis and the natural bone. A good bone cement is expected to be biocompatible, have high mechanical strength, have the low curing temperature as much as possible, and transmit the applied load to the bone homogeneously. In this study, PMMA-based cement formulations were prepared, and modifications were made by adding bioactive glass-ceramic to the formulations to increase mechanical strength, thermal properties and biocompatibility. The prepared cement's mechanical, thermal, and biological properties were investigated, and the results are below.

5.1. CHARACTERIZATION OF BIOACTIVE GLASS-CERAMIC

5.1.1. Thermal Analyses Test Results

The mass loss or gain upon heating BGC to temperatures up to 1000 °C was determined using thermogravimetric analysis. The TG curve in Figure 5.1 shows that at concentrations of 1, 3, and 5 percent vanadium, the weight decreased by 24%, 21%, and 17%, respectively, over two periods. First, the water and OH groups were removed between 25°C to 210°C, 25°C to 260°C, and 25°C to 300°C, respectively, resulting in weight loss [100, 101]. In the second stage, the range between 550 °C and 700 °C indicated the beginning of the crystallization process in all samples. X-ray analysis revealed a temperature over 800 °C was required to melt the crystalline phase [102, 103]. Previous investigations indicate that the phase change in BG starts at a temperature of 732 °C. Therefore, the sintering temperature was set at 800°C to allow this research to compare crystallinity, biomineralization capacity, and biocompatibility in vitro.

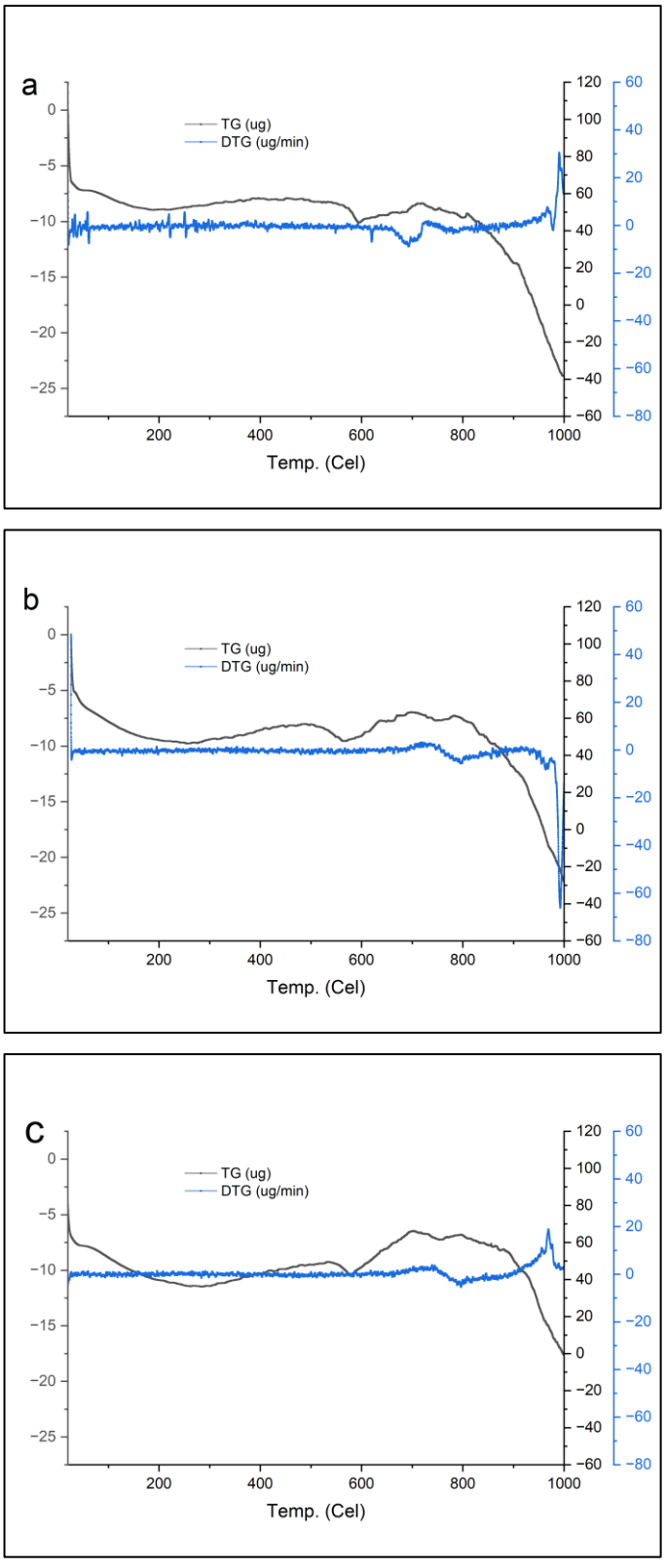

Figure 5.1. Thermal analyses of samples a) SCNBV1, b) SCNBV3, c) SCNBV5, from 25 °C to 1000 °C.

5.1.2. XRD Analysis

Figure 5.2 shows the XRD patterns of the bioactive glass-ceramic samples before and after soaking in SBF for 7, 14, and 21 days. According to the standard JCPDS maps, two new peaks found at 32 and 26 degrees were identified as (211) and (002) apatite (002-0647). After the 7-day immersion period, the two peaks increased, and two more apatite peaks also appeared at 45.5 and 48.5 degrees. After being submerged for 14 days, all of the peaks appeared identical. On the first day, the amorphous samples showed a peak at 32 °C, and its intensity decreased after soaking in SBF solution due to the formation of a hydroxyapatite layer on the surface of the sample, resulting in a decrease in intensity of the peak [104]: The crystal size and the amount of strain in the lattice affected the width of the XRD pattern. An imperfect crystal had a smaller base and a broader apex.

The XRD pattern showed a significant apatite-wide reflection, indicating excellent crystalline phase formation. It could be argued that V_2O_5 could get into the still-forming apatite nuclei, preventing them from developing into the large apatite crystals that would otherwise form because the apatite structure would not be able to accommodate it. The introduction of V_2O_5 into the apatite lattice affects the physicochemical properties of the mineral. Importantly, inorganic ions such as vanadium ions prevent the crystallization of apatite and, at higher concentrations, allow the formation of amorphous calcium phosphate. These conditions could accelerate apatite agglomeration [105].

When examining the precipitates in the bioactive glass ceramic, the lattice constants increased linearly since apatite was quantitatively combined with the element boron. These changes were consistent with the fact that the ionic radius of calcium is smaller than that of boron. In light of the explanations, the XRD patterns and FTIR spectra indicate the formation of a small number of low-crystalline calcium phosphate (HA) crystals. This indicates that the peaks of the XRD pattern and the FTIR bands are properly separated [31, 106, 107]. The obtained results proved that adding V_2O_5 content in the glass network enhanced the formation of the apatite layer.

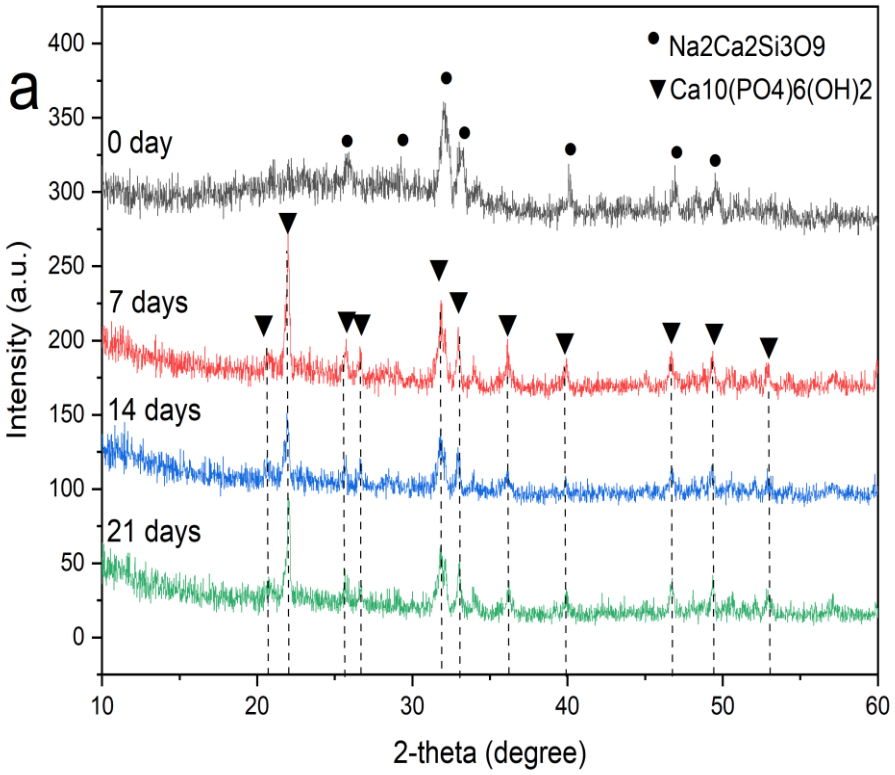
a
Na2Ca2Si3O9
Ca10(PO4)6(OH)2
0 day
7 days
14 days
21 days
Intensity (a.u.)
2-theta (degree)
0
50
100
150
200
250
300
350
400
10
20
30
40
50
60

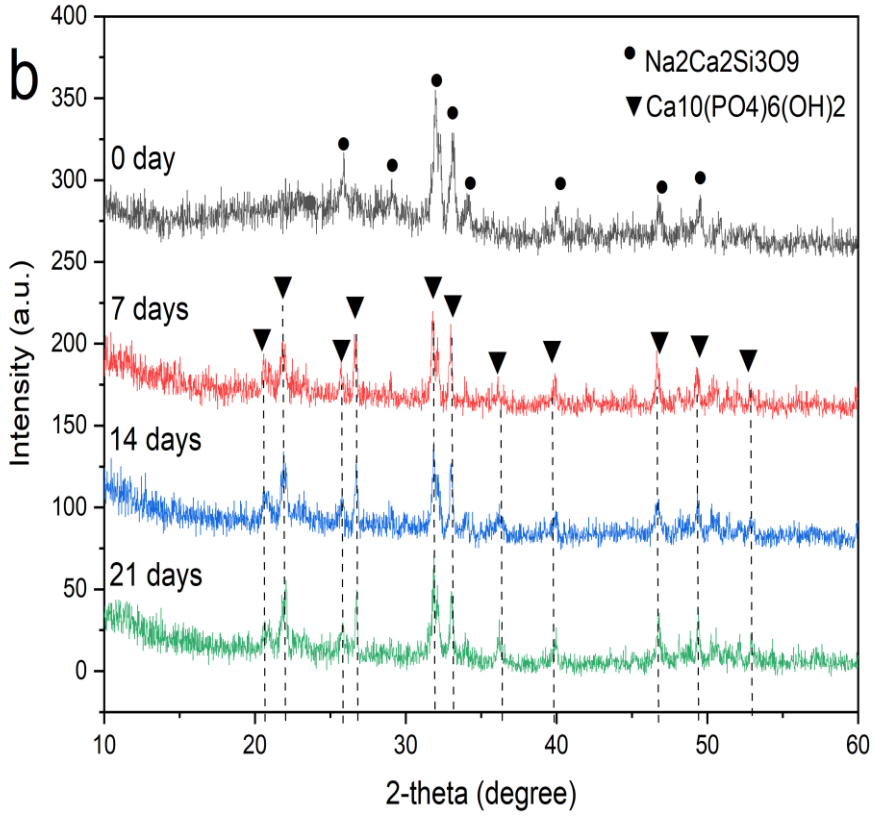
b
Na2Ca2Si3O9
Ca10(PO4)6(OH)2
0 day
7 days
14 days
21 days
Intensity (a.u.)
2-theta (degree)
0
50
100
150
200
250
300
350
400
10
20
30
40
50
60

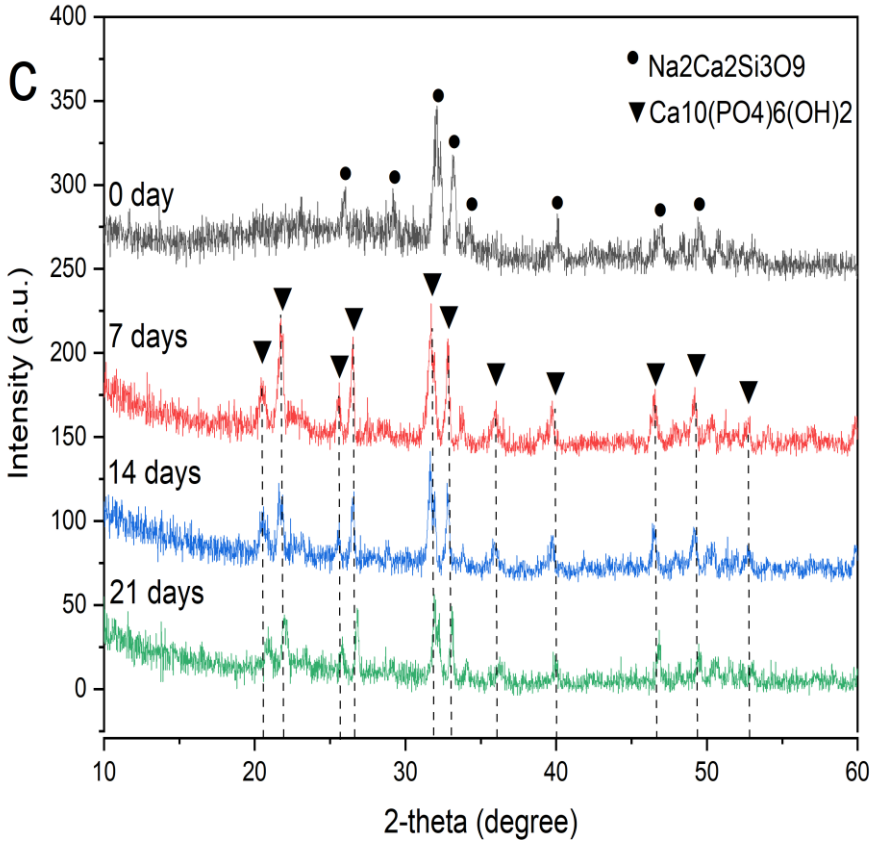

Figure 5.2. The bioactive glass sample's X-ray diffraction patterns before and after SBF immersion. (a SCNBV1, (b) SCNBV3, (c) SCNBV5.

5.1.3. FTIR Result

According to the results of FTIR, there seems to be a connection between the formation of a clustering process in highly modified glasses and non-bridging oxygen atoms (NBOs) when silicate networks (rich silicate glasses with a modifier) are prepared. The results of this study support the existence of a specific form of bridging oxygen (BO). [108, 109] can form a cluster of sodium atoms by bridging two sodium atoms together. A correlation was found between the total NBO atomic concentration and the NBO atomic concentration in the silicate glass matrix. If so, they are glasses that contain many modifiers of a specific type. Hence, forming a crystalline phase in NBO requires a specific class of structural species to be present. It has been said that the formation of aggregate species is a crucial factor in making materials more bioactive [110, 111].

Crystalline wollastonite (calcium silicate, $CaSiO_3$), apatite (calcium phosphate), and Na_2VO_3 species are studied using FTIR spectroscopy to learn more about the structure of Na_2O-CaO-SiO_2-V_2O_5 glasses. The fully formed species are considered the most valuable and essential and are responsible for the majority of the bioactivity of the material [112].

The FTIR spectra of all glass samples are shown in Figure 5.3. The FTIR reflection spectra of the bioactive glass-ceramic samples all show distinct bands, showing that they all consist predominantly of a silicate network. This behavior would be expected when SiO_2 is an essential component of glass. There was a consistent pattern across all bioactive glass-ceramic samples. Therefore, the bioactive glass-ceramic shows peak values at 789, 950, 1050, 1390, 1440, 1720 and 3736 cm^{-1}. Infrared spectra from this process showed peaks at 789 cm^{-1}, indicating a symmetric bending mode between Si-O-Si and Si-Si and a band at 950 cm^{-1} corresponding to vibrational bending modes [31]. The band at 1050 cm^{-1} corresponds to the Si-O-Si bond associated with a symmetric stretch of non-bridging oxygen atoms within tetrahedral structures. Due to these considerations, the band's intensity is restored by incorporating vanadium oxide into the base glass. It follows that vanadium oxide increases the proportion of oxygen that does not form a bridge in the network [113].

The BO vibrational mode was identified at a frequency of 1390 cm^{-1}. The absorption of the carbonate group was assumed to be in the range of 1420- 1455 cm^{-1}. The C-O vibrational mode was assumed responsible for the band observed at 1720 cm^{-1}. Researchers found that more vanadium oxide resulted in a more substantial IR peak. The vanadium oxide caused the Si-O-Si network to break down [114].

This proves the presence of infrared frequencies and the associated functional and structural groups in the bioactive glass-ceramic. The bioactive glass-ceramic IR spectral bands with vanadium oxide as a substitute show no discernible changes [115].

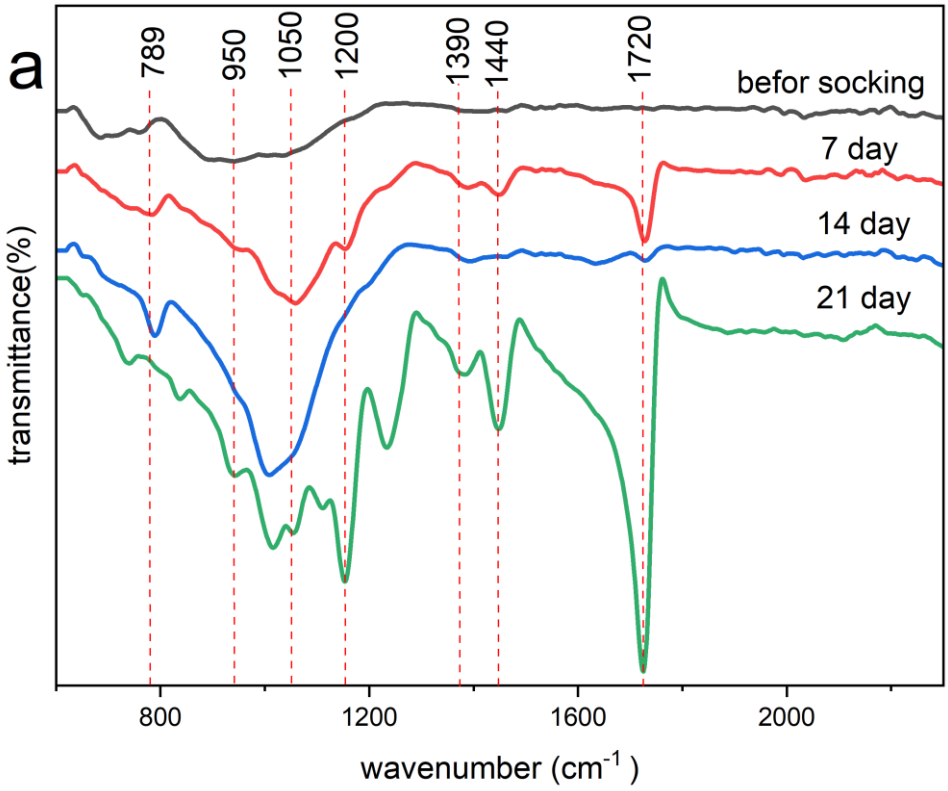
a
789
950
1050
1200
1390
1440
1720
befor socking
7 day
14 day
21 day
transmittance(%)
800
1200
1600
2000
wavenumber (cm-1)

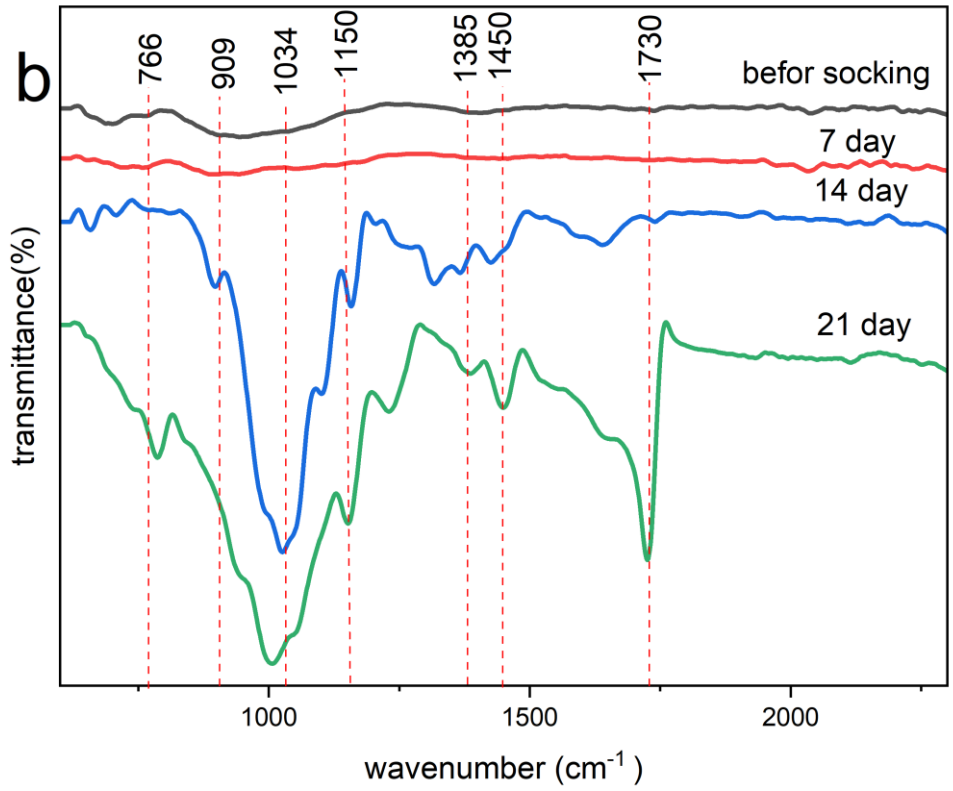
b
766
909
1034
1150
1385
1450
1730
befor socking
7 day
14 day
21 day
transmittance(%)
1000
1500
2000
wavenumber (cm-1)

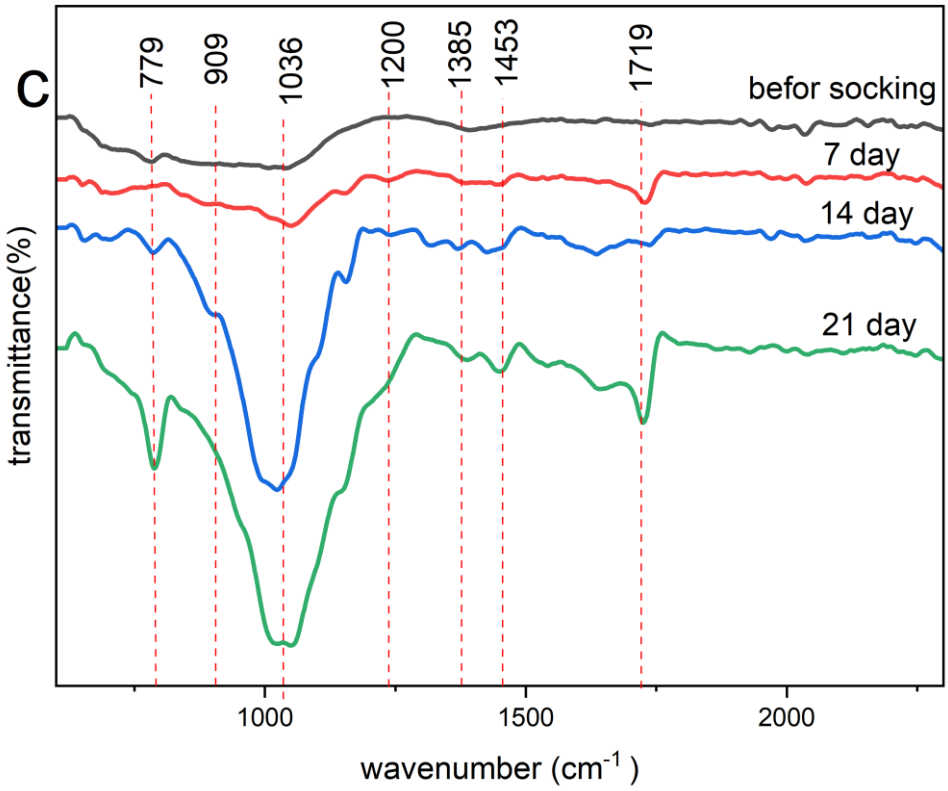

Figure 5.3. FTIR spectra of prepared glasses before and after immersion in SBF for a) SCNBV1, b) SCNBV3, and c) SCNBV5 for 0, 7, 14, and 21 days of soaking.

5.1.4. SEM Analysis

Figure 5.4 (a-e) shows scanning electron micrographs (SEM) of SCNBV samples taken before and after in vitro testing. Figure 5.4 (a) is a scanning electron micrograph of three vanadium-concentrated samples showing a smooth, layer-free glass surface. The SEM images of the SCNBV glass surface after 21 days of immersion in SBF showed surface precipitation in a spherical cluster configuration. Brauer et al. [107] show that surface precipitation on a bioglass sample is the main factor in developing the HAp layer. The SEM image shows that the surface of the cleaned and tempered glass is covered with HAp particles. The degradation of Ca and P ions after 21 days in SBF leads to forming of the HAp layer on the glass surface. The formation of a HAp layer on the glass surface creates a stable adhesion to the host tissue. Due to the structural similarity of HAp to bone, osteointegration

can occur. Therefore, bone binding and bioactivity capacity are related to forming a HAp layer on the glass surface. It was found that glass samples with higher bioactivity showed more development of the apatite layer [116].

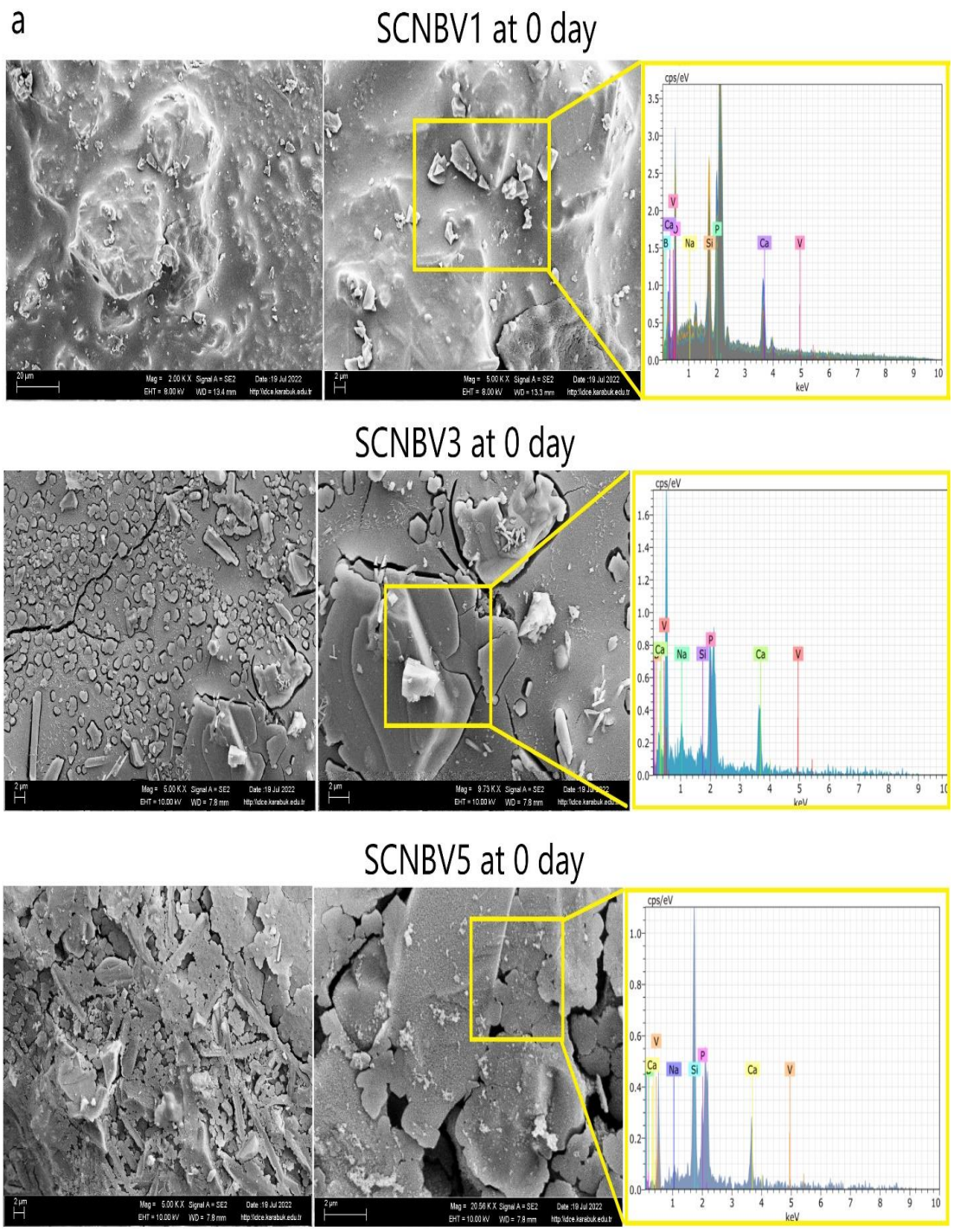

b

SCNBV1 at 3 days

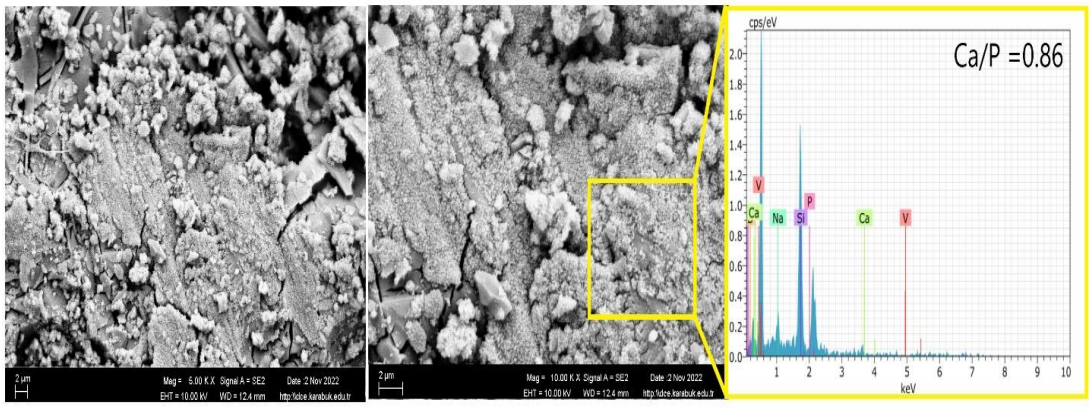

SCNBV3 at 3 days

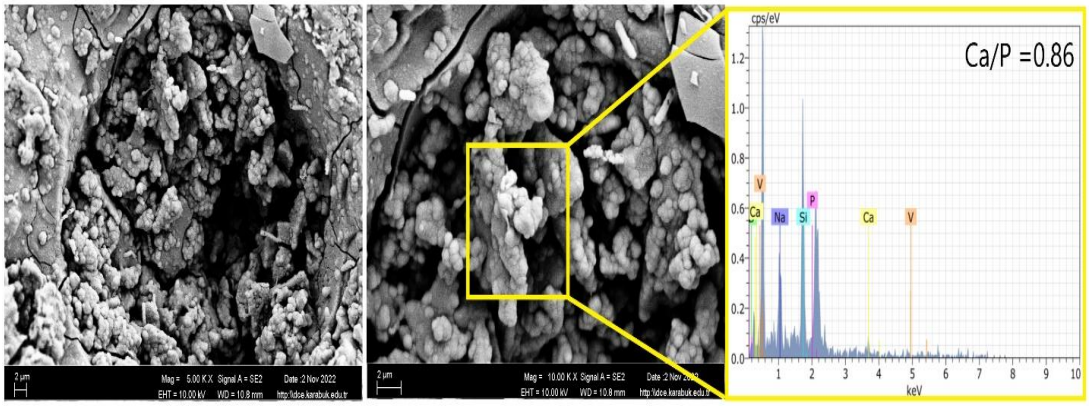

SCNBV5 at 3 days

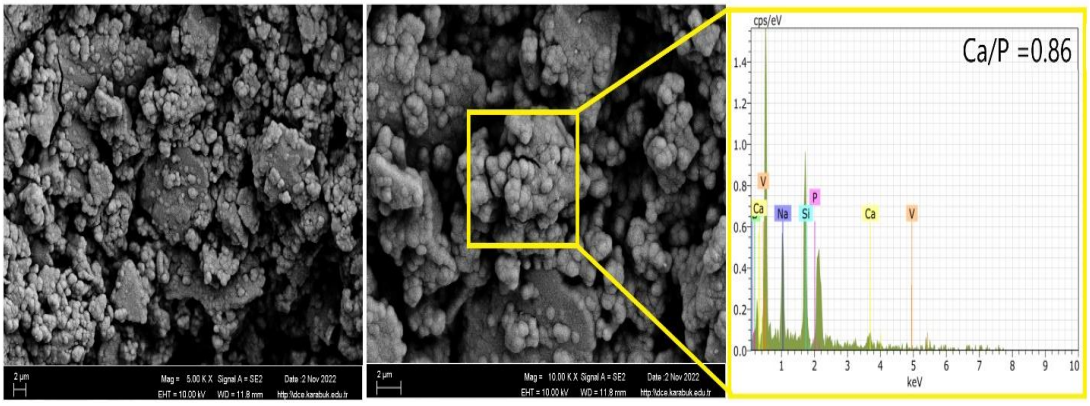

C

SCNBV1 at 7 days

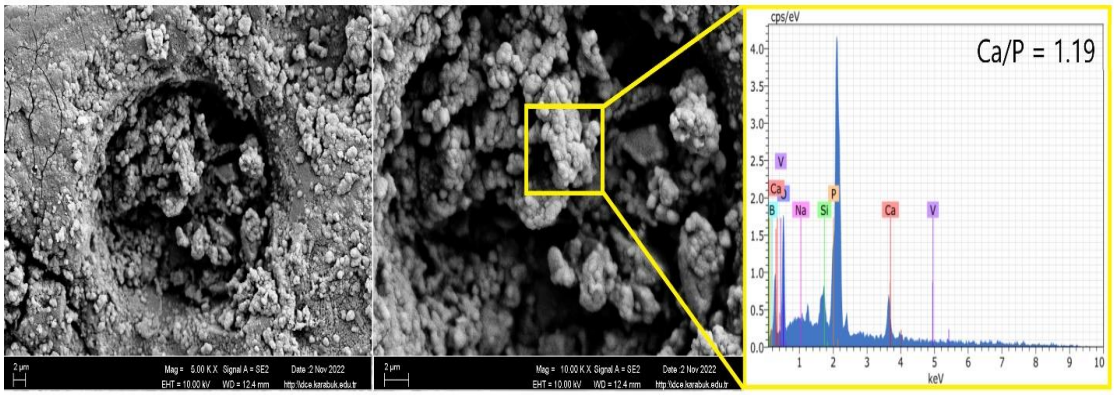

SCNBV3 at 7 days

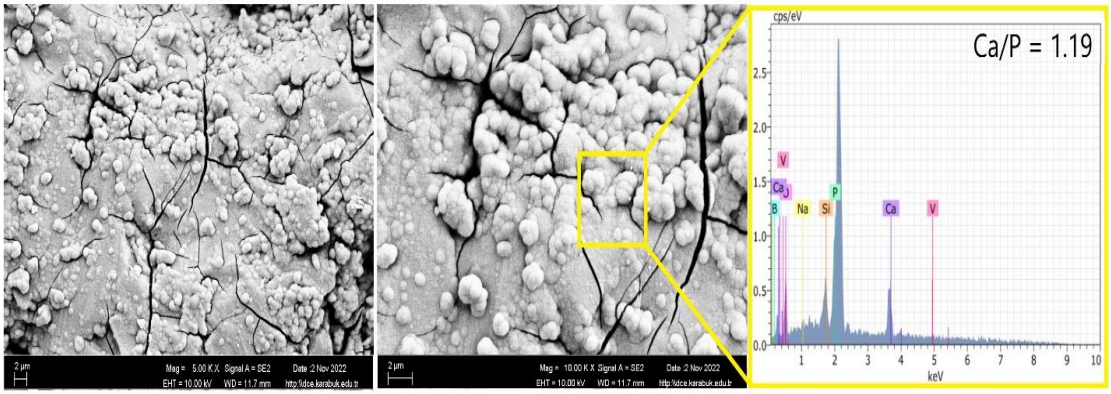

SCNBV5 at 7 days

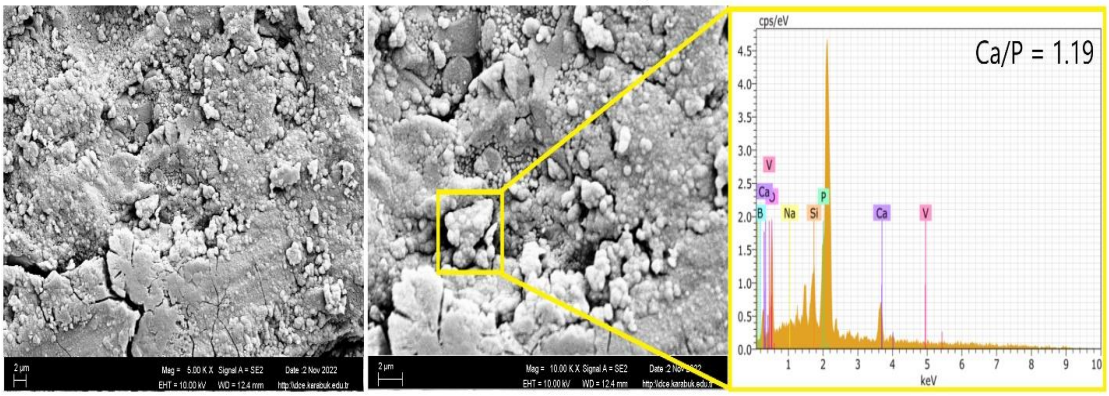

d

SCNBV1 at 14 days

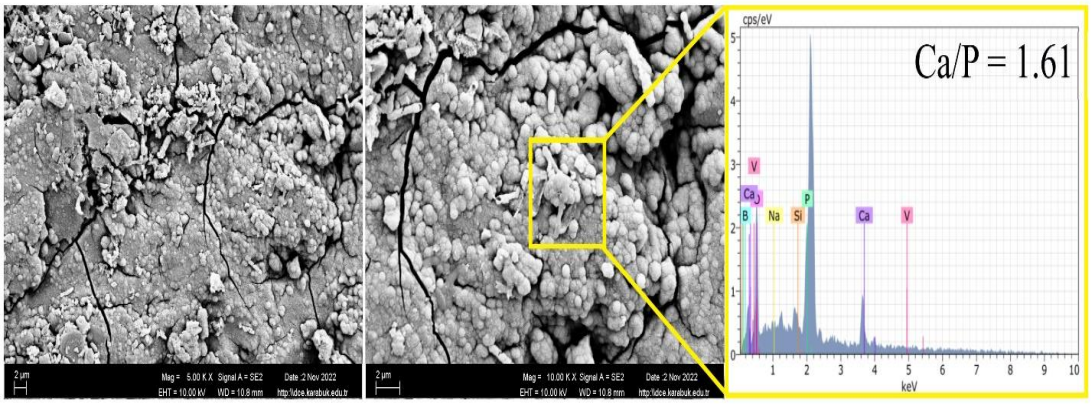

SCNBV3 at 14 days

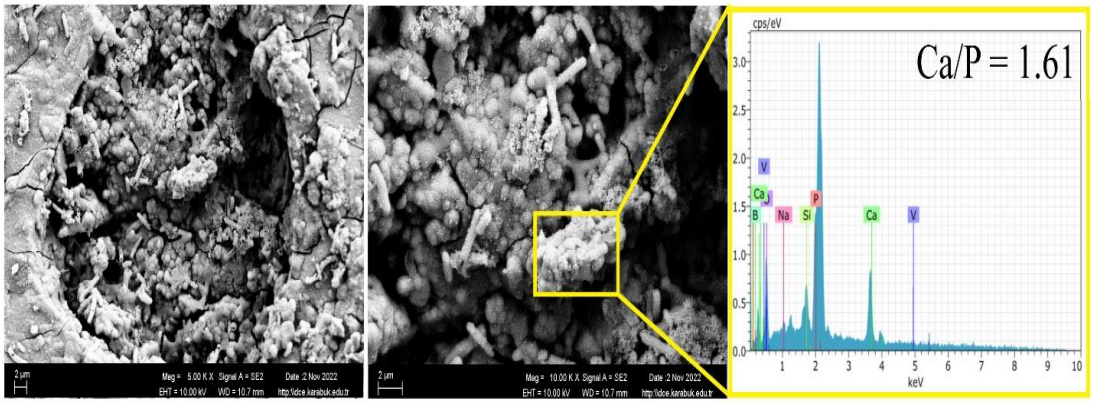

SCNBV5 at 14 days

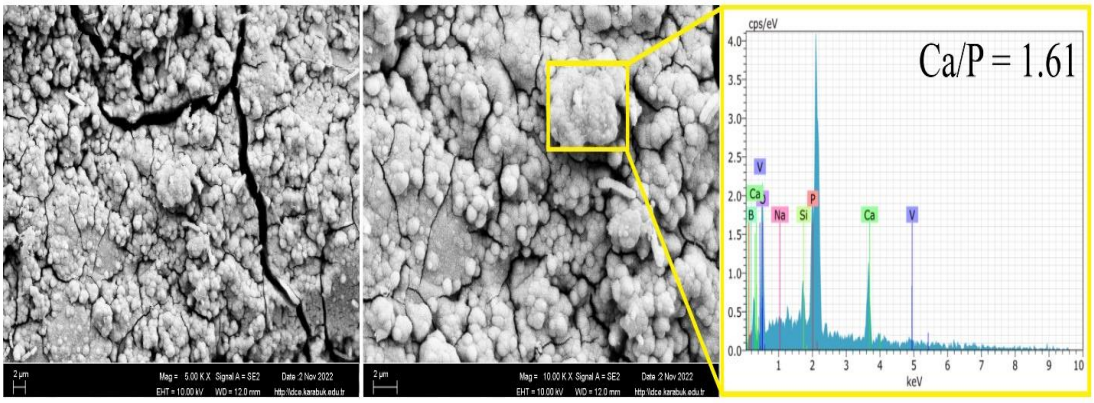

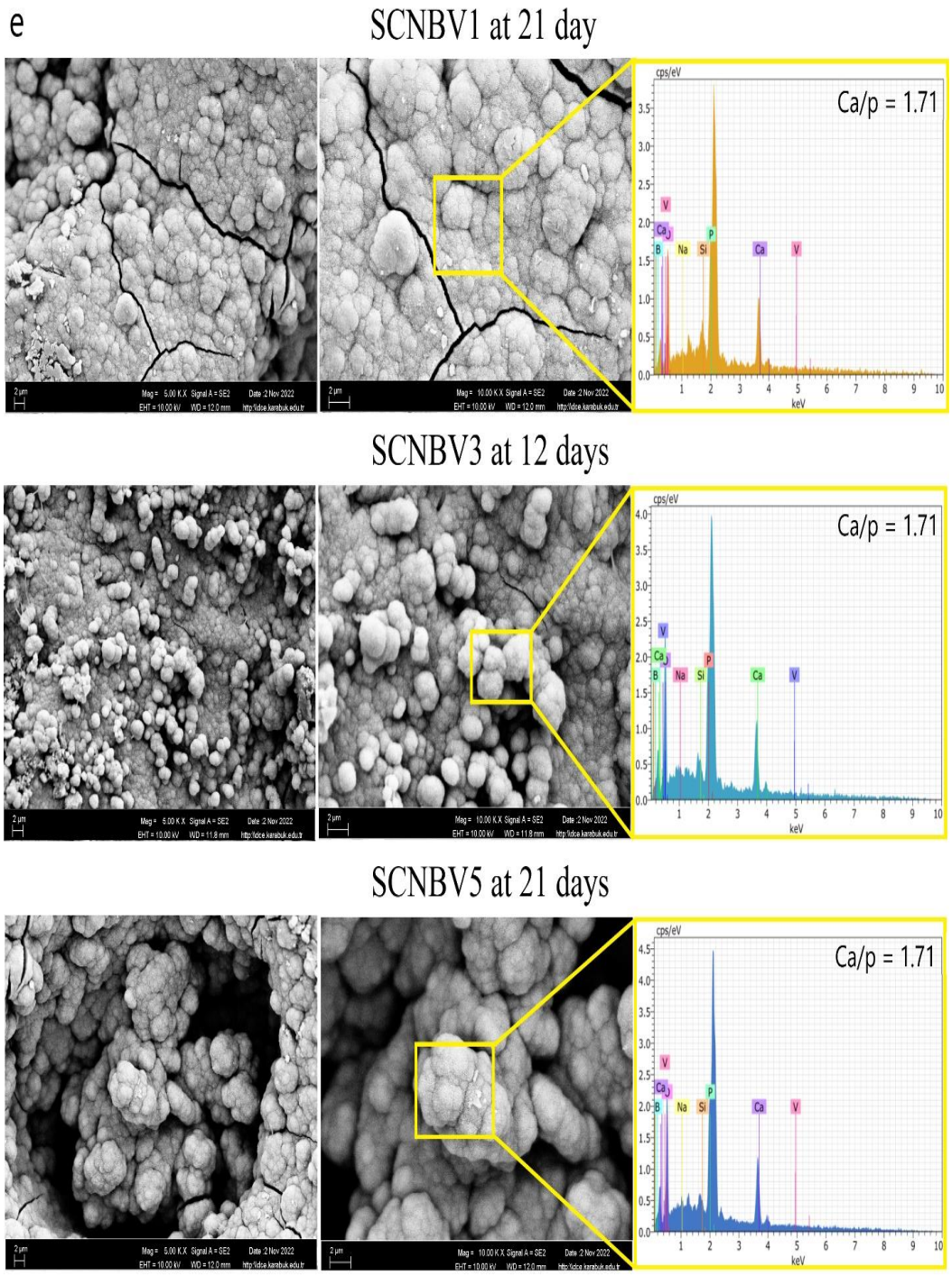

Figure 5.4. Morphological properties of glass-ceramic a) before immersion at SBF, b) immersion at SBF for 3 days, c) immersion at SBF for seven days, d) immersion at SBF for 14 days, e) immersion at SBF for 21 days.

Using an energy dispersive X- spectrograph (EDX), the elemental composition of the glass samples was analyzed both before and after 21 days of immersion in SBF. All samples contained the expected ions, including Si, Na, P, B, Ca and V, according to

EDX analysis [117]. The glass samples were also tested and found to be pure. Elements are lost during the glass melting process, which explains the small gap between the experimental and nominal compositions. A Ca/P atomic ratio of about 1.67 was calculated for the glass samples, corresponding to the typical hydroxyapatite value [118]. Scanning electron micrographs taken of the treated glass samples showed evidence of the development of an apatite layer. Furthermore, as shown in sections 5.2 (XRD results) and 5.3 (FTIR results), there was a strong correlation between the results and the XRD and FTIR studies.

5.1.5. PH and weight loss analysis

After soaking in the SBF solution, the glass-ceramic samples were subjected to a series of tests to determine how they would degrade. Figure 5.5 shows how the SBF solution's pH changed over the experiment and how much weight the BG sample lost. A steep increase in pH is observed after seven days of immersion in the SBF solution. After immersion, alkaline ions such as Na^+ and Ca^{2+} are released into the SBF, lasting 7 to 21 days. This makes the SBF easier. This increases the pH of the remaining SBF. The fact that the pH increases shows that Ca^{2+} ions are released into the solution. When BG samples are added to the SBF solution, these ions briefly swap places with H^+ ions [119, 120]. In BG samples, these ions briefly swap places with H^+ ions. Because these samples have many pores and are very reactive, the mesopores accelerate ion exchange. This exchange increases the pH of the solution [121].

By measuring the weight of the decomposed glasses, we may learn more about the speed at which glass dissolves in liquids thought to represent blood and other bodily fluids. Figure 5.5 shows the relationship between time and weight loss. The weight loss steadily increases throughout the experiment with the increasing time that bioactive glass-ceramic samples are immersed in SBF. Even if the sample weight loss rate increases over time, the overall trend is still downward. A. For example, glass-ceramic samples lost up to 14% of their original weight after one week of immersion in amorphous bioglass. Then they lost another 8% of their weight between week 13 of the experiment. As the dissolution process progresses, ion exchange between the glass sample and the SBF increases, and the bioactive glass-

ceramic surface leaches through contact. Ca/P forms an amorphous layer when exposed to water [122].

As the incubation time increases, a crystallization layer forms on the surface. This protective layer prevents surface degradation and promotes the growth of a crystalline HA surface. Because of these drastic pH changes, producing apatite that mimics bone requires the weight loss the developed bioglasses entail. The mineralization of the glass-ceramic surface is due to several processes, including those that lead to a weight loss of the sample and those that cause a shift in the pH of the solution [123]. Dipping in SBF can turn bioglass-derived materials into something resembling apatite. The importance of this property has been hotly debated for a long time. As the 45S5 bioglass crystallized, the previously bioactive glass-ceramic became non-living in her research on glass-ceramics crystallization [124]. Previous studies found that the crystallization process did not prevent the formation of an appetite layer.

Nevertheless, this process was delayed by 10 to 22 hours. A calcium phosphate layer was formed after a sample of sintered 45S5 crystalline bioglass was immersed in simulated body fluid (SBF). Figure 5.5 shows the glass and ceramic samples analyzed for their mineral content in relation to the soaking time in SBF.

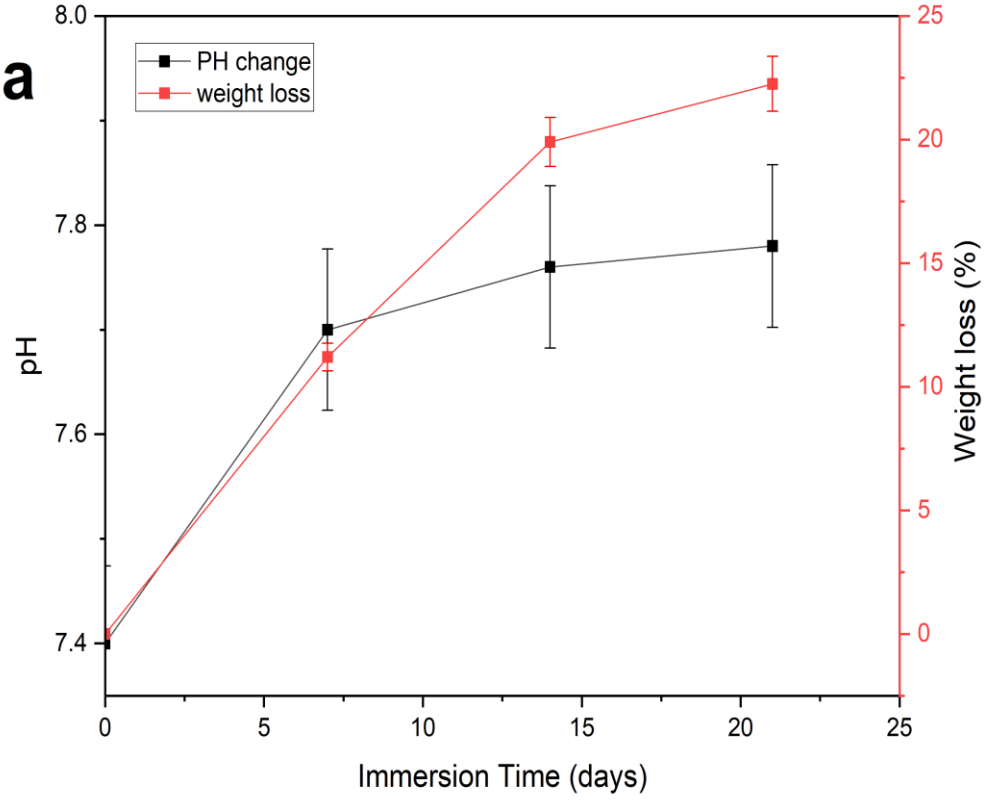
a
PH change
weight loss
pH
Weight loss (%)
Immersion Time (days)
8.0
7.8
7.6
7.4
25
20
15
10
5
0
0
5
10
15
20
25

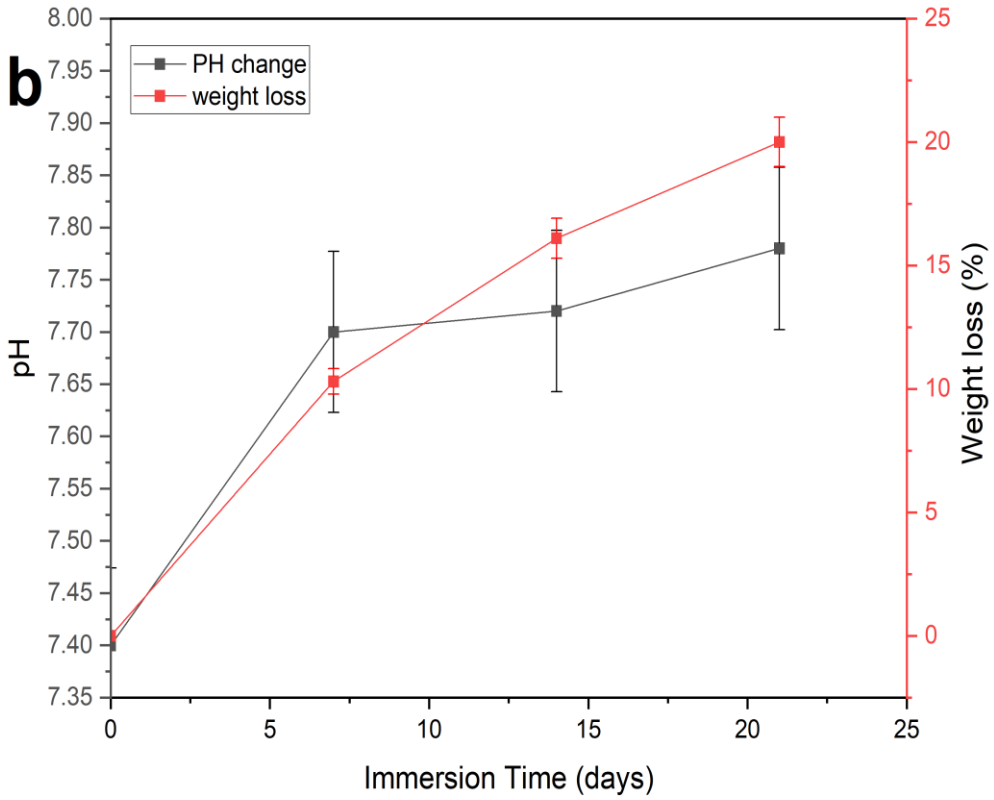
b
PH change
weight loss
pH
Weight loss (%)
Immersion Time (days)
8.00
7.95
7.90
7.85
7.80
7.75
7.70
7.65
7.60
7.55
7.50
7.45
7.40
7.35
25
20
15
10
5
0
0
5
10
15
20
25

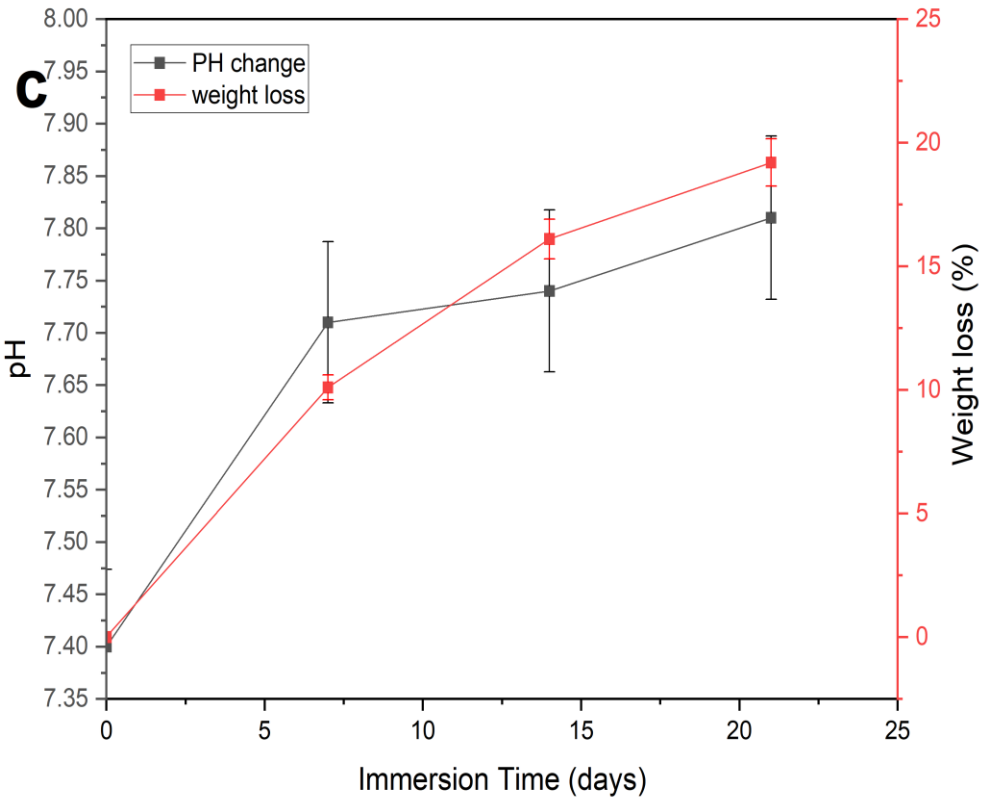

Figure 5.5. Analysis of PH and weight loss of the glass-ceramic during SBF immersion a) SCNBV1, b) SCNBV3, c) SCNBV5.

5.2. CHARACTERIZATION OF BONE CEMENT

5.2.1. In vitro analysis

Figure 5.6 shows the XRD patterns of PMMA and bone cement with different concentrations of the prepared bioactive glass (0.10 and 20% by weight) after soaking in SBF for 7 days. It was found that the apatite peak was clearly generated on the glass-ceramic surface at 2=22.5, 32.3 and 33. It is assumed that the proportion of glass ceramic in the cement is insufficient. This could be due to the high viscosity of the mixture, caused by the addition of fillers during the mixing process, which led to an uneven distribution of the glass ceramic in the cement sample [99]. The combination of uneven filler distribution and small sample size can result in the XRD failing to identify the apatite signal. Goto et al. [125] discovered that adding 50–56 wt% bioactive titanium dioxide particles to PMMA bone cement increased its

osteoconductive and mechanical properties. Renteria-Zamarron et al. [126] discovered that the addition of 39 and 49 wt% wollastonite to PMMA bone cement increases bioactivity through the formation of an apatite phase on XRD peaks and the generation of a thick and homogeneous ceramic layer on cement samples. It is evident that adding small amounts of glass-ceramic fillers does not lead to bioactive PMMA bone cement.

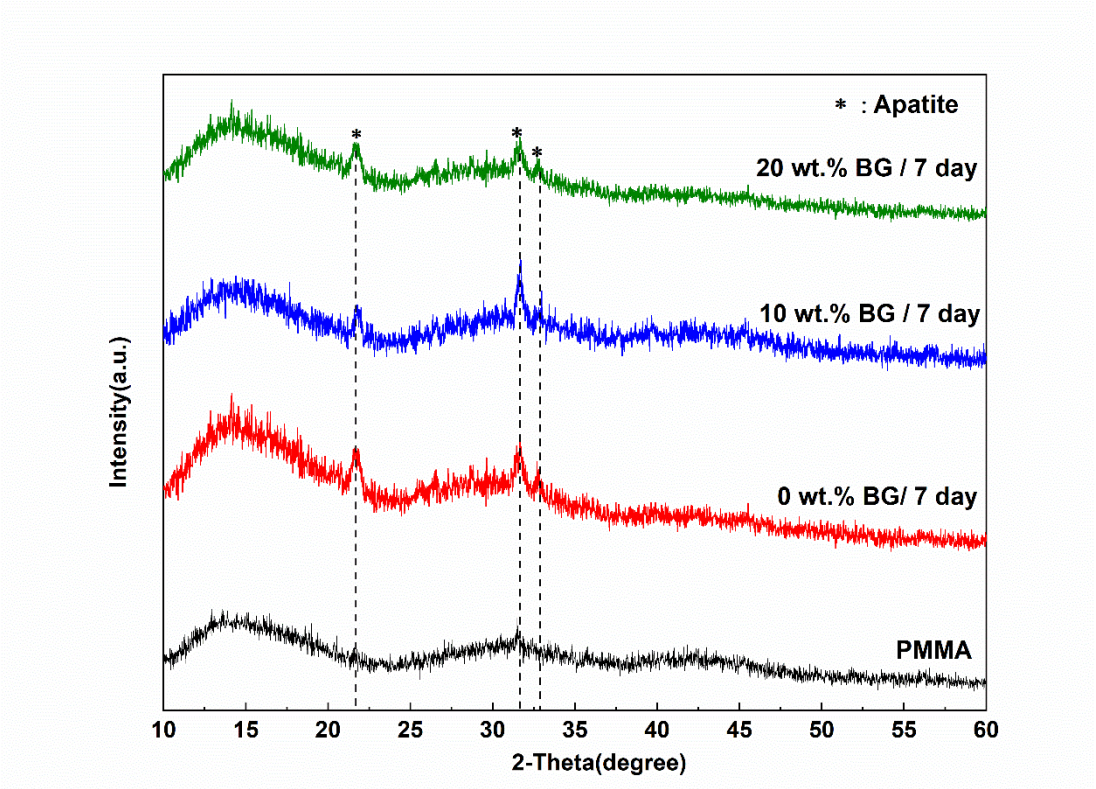

Figure 5.6. XRD patterns of Bone cement before and after soaking in SBF for 7 days.

Bone cement is crucial in orthopedic surgeries to secure implants and stabilize fractured bones. It is instrumental in ensuring the success and longevity of these procedures. However, it is essential to understand bone cement weight loss after immersion in simulated body fluid (SBF). The potential impact of weight loss on the stability and longevity of orthopedic implants makes it necessary to study bone cement degradation behavior in SBF. This research contributes to the overall effectiveness and reliability of orthopedic procedures by ensuring patient safety and successful surgical outcomes. The weight loss after 7-day immersion in SBF was 0.34%, 1.46%, and 1.97% for neat PMMA, 10% BG, and 20% BG, respectively, as shown in Figure 5.7 (a). The pH results for samples immersed in SBF after 7 days at

37°C are shown in Figure 5.7(a). Figure 5.7(b) shows the pH profile of the SBF solution during 7 days of immersion. The control sample of PMMA does not follow the same trend as the other samples. The pH of PMMA increased slightly after 7 days of immersion, which is most likely due to the formation of OH. Samples with added bioactive glass-ceramic showed a higher pH than fresh SBF. However, the largest and smallest growth can be observed for the pH value and PM. The precipitation of calcium (Ca) and phosphate (P) on the surface of the bioactive glass composite with PMMA could be responsible for the initial pH increase [127].

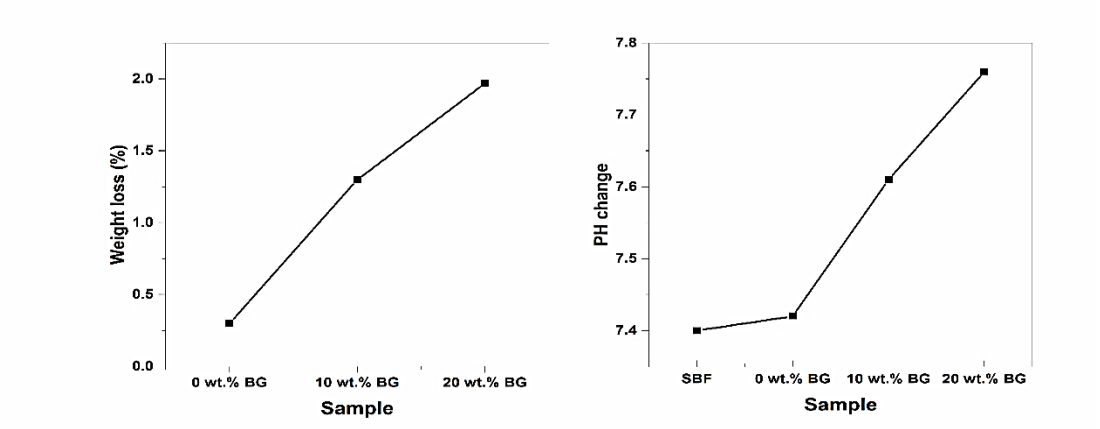

Figure 5.7. Immersion test of samples in SBF for 7 days at 37 ℃ (a) weight loss and (b) ph change.

5.2.2. Mechanical properties

As a cement, PMMA used in surgery tends to crack easily. In the same way that other brittle materials are weak in tension but strong in compression, this one may succumb to uniaxial compression. Measurements of compression yield strength values of the produced cement are crucial [30] since compression is the major direction of strain on bone cement in a complete hip implant. The findings showed that the ultimate tensile strength and elastic modulus were highest in PMMA cement containing 10% bioactive glass. This set also included the lowest measured elongation-at-break value. Figure 5.8 shows the decrease in ultimate tensile strength and elastic modulus found when HA was added at a concentration of more than 10 wt%.

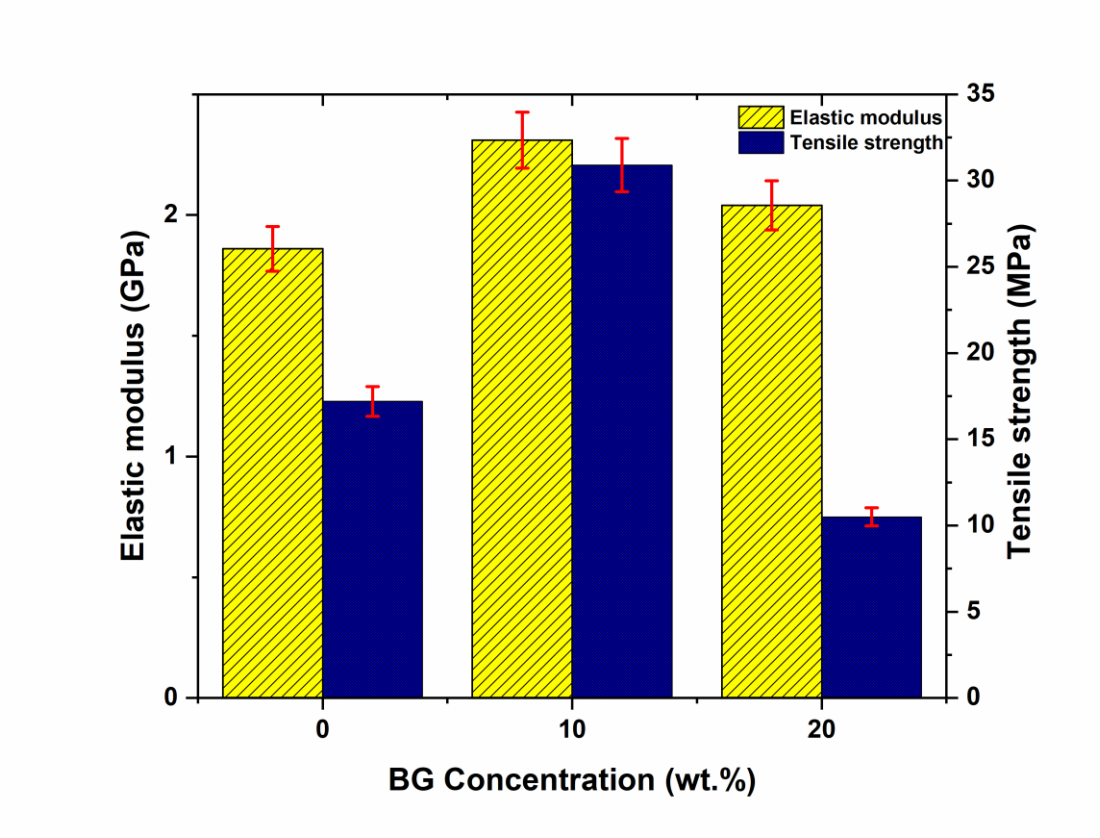

Figure 5.8. Mechanical properties data for the tested samples.

For the compressive strength, the result shows that the compressive strength decreases with increasing the concentration of bioactive glass; Figure 5.9 shows the cement samples' typical values of ultimate compressive strength.

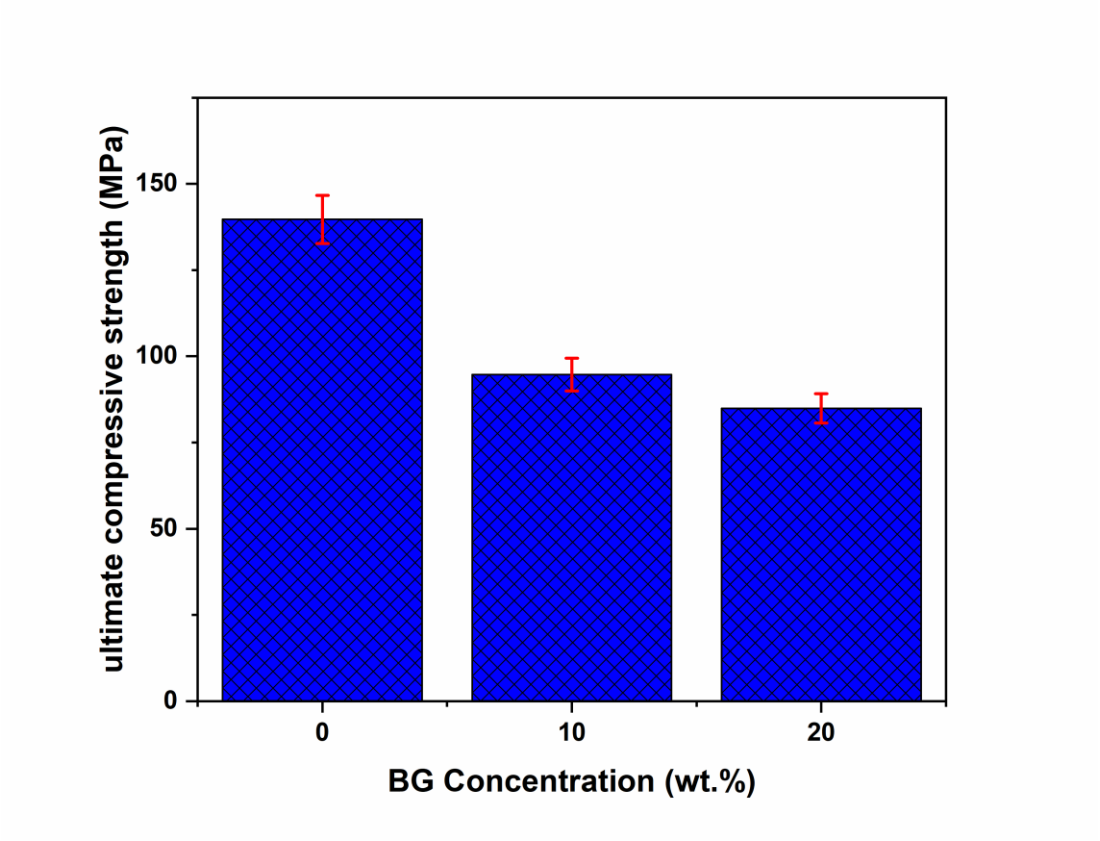

Figure 5.9.Compressive strength for the bone cement samples.

Ultimate compressive strength decreases with increasing filler loading and average particle size for most, but not all, composites. The reduction in compressive strength and compressive yield point is explained below. Since the shrinkage of the PMMA matrix is greater than the shrinkage of the bioactive glass particles during the setting and cooling step, the bioactive glass particles are securely encapsulated and compressed in the PMMA matrix. This creates a circumferential tensile stress in the bone cement matrix next to the bioactive glass particles. This hoop stress reproduces a weak bond between additive particles and the PMMA matrix [128]. When loaded, the additive particles form a second phase in the continuous phase of PMMA, and the interface between the two phases acts as a grain boundary, preventing cracking. A frictional force is created at the edges of the fracture, which opposes the force that initiates the crack. The belt tension remains at this point, but the magnitude of the frictional force is probably more significant than the circumferential force. The hoop stress contributes to separating the fracture edges [128]. Due to the poor bonding

area between these two phases, the ultimate compressive strength and compressive yield strength can be reduced.

Furthermore, this is consistent with the results that adding bioactive glass without any chemical treatment reduced the mechanical strength of the bone cement. The degree of adhesion between the bioactive glass particles and the matrix could explain the observed printing behavior. Poor component adhesion reduces yield strength as if the system were void filled. When bioactive glass particles are present in moderate concentrations and evenly distributed in the cement paste (as in the PMMA-2.5HA sample), they act as charge carriers and result in excellent mechanical properties. If the proportion of bioactive glass particles increases, an inhomogeneous distribution and, as a result, particle aggregation can occur. This can lead to phase separation, inhomogeneity in structure and poor adhesion to the matrix, reducing compressive strength [128].

5.2.3. Setting time

One of the cement's most important handling properties is its setting time, which varies depending on the composition, mixing environment, and additives [129]. When used in the clinical study, the composite bone cement was injected before the final setting time, and the incision was closed. The main reason for bone cement's rapid setting and strength is its hydration product in a solid network [130]. Due to the fast reaction, PMMA was combined with bioactive glass in this study to accelerate the hydration of the mixtures [131]. Table 5.1 indicates the mean value of setting time (t_{set}) and temperature (T_{set}) as well as the highest polymerization temperature (T_{max}) and time (t_{max}) measured.

In this study, cement with a fast setting time were developed. On the other hand, cement with a short setting time minimizes the complication rate, enables faster wound closure and saves operating time [132]. However, setting time may be short and operative time insufficient; thorough planning and assessment of the defect before cement preparation and application allow the surgeon to overcome this problem. The result shows that the maximum temperatures were between 53 and 42 °C. All filled bone cement samples had lower peak temperatures than the control sample (PMMA without bioactive glass). Increasing the filler loading or decreasing

the L/P ratio decreased the peak temperature of PMMA bone cement composites. Small exotherms can be attributed to glass ceramics, as ceramic materials act as thermal insulators, absorbing some heat generated during the polymerization reaction [99]. Although the peak temperature drop is insignificant, it can be attributed to glass-ceramic presence. Instead, increasing the glass in the assembly increases the time required to reach the optimum temperature. Increasing the amount of glass confirms a delay in the polymerization kinetics, as already observed by other researchers [99, 133]. However, the parameters acquired comply with ISO requirements (between 3 and 15 minutes for set and a maximum temperature of 90 °C). This was suggested by Jasso-Gastinel et al. suggested. [134] that it is preferable to have some leeway for manipulation before the cement sets. Since it is necessary to maintain pressure in the prosthesis while waiting for the cement to set, complications can arise if the setting time is too long. Shortened dough time at higher filler loading may be due to the increased viscosity of the mixture that occurs during the setting and incorporation of fillers. When using acrylic bone cement in the operating room, the dough time is critical as it indicates when the cement can be delivered without sticking to the surgeon's glove [135]. However, this technique is highly dependent on the operator's skill and can be somewhat arbitrary.

Table 5.1. Curing parameters of composite bone cement with different proportions of glass particles

Filler loading (wt.%)	**L/P ratio**	**T_{max} (°C)**	**t_{max} (min)**	**T_{set} (°C)**	**t_{set} (min)**	**Dough time (min)**
0	0.5	53	10.3	41	10	4.50
10	0.45	48	12	41.5	11.5	3.32
20	0.41	42	14	43.5	13	4.18

PART 6

CONCLUSIONS AND RECOMMENDATION

6.1. CONCLUSIONS

In this work, the synthesis and characterization of modified bioactive glass ceramic and its effect on the bone cement based on PMMA were investigated, and the results obtained allow us to state the following conclusions:

i. The melting point of the glass decreased from 1400 °C to 1100 °C due to the substitution effect with 15% B_2O_3 and X% V_2O_5 (X = 1, 3 and 5).

ii. In synthesizing the sodium calcium silicate crystal $Na_2Ca_2Si_3O_9$ used in the glass-ceramic preparations, we mixed the ingredients in a large vat, heated to 1100°C, cooled rapidly in water and then sintered at 800°C.

iii. After seven days in SBF, the crystalline $Na_2Ca_2Si_3O_9$ on the surface almost completely transformed into the amorphous calcium phosphate known as carbonated hydroxyapatite

iv. Since the functional groups C-O and P-O were present at different times, HCA layers could form. Based on SEM and EDX analysis, hydroxyapatite (HA) and HCA cluster crystals started forming on both glass-ceramic surfaces on day 3 and day 21.

v. SEM images showed good growth of hydroxyapatite on the surface of the samples. EDS examination of the surface of the immersed samples showed the precipitation of calcium and phosphorus elements at a percentage of 1.61, which is close to the Ca/P ratio of natural bone.

vi. During the dissolution process, the weight of the sample decreased as Ca^{2+} and PO_4^{3-} ions were released from the glass matrix into the SBF solution. It was hypothesized that an intermediate vanadium ion formed BO_3 groups in a triangular shape, which loosened the borosilicate glass network. Bioactive

vii. borate and V_2O_5 glass ceramics are good candidates for use in medical applications.

viii. In the last part of this study, bioactive glass was used as an additive. PMMA/BG bone cement composites were successfully fabricated in this study. The materials were accurately characterized using XRD and in vitro analysis; The presence of bioactive glass was confirmed by XRD. The addition of 10-20 wt% BG led to (a) a reduction in the setting time of cement and (b) an improvement in mechanical properties.

6.2. RECOMMENDATIONS

The results obtained in the course of this investigation allow us to suggest the continuation of studies through the following lines of complementary research:

i. The use of other oxides with a low melting point and good properties and the formation of a eutectic compound to reduce the melting point to a large extent, for example, boron oxide with potassium oxide.
ii. Study the Antibacterial behavior of the prepared bone cement
iii. Change the proportion of the mixture and carry out new tests to expand the knowledge and application of this promising bone cement.
iv. Study the biocompatibility for the prep read bone cement

REFERENCES

1. Pal, S., *Design of artificial human joints & organs*. Vol. 1. 2014: Springer.
2. Mistry, A.S. and A.G.J. Mikos, "*Tissue engineering strategies for bone regeneration"*. **Regenerative medicine Ii: clinical preclinical applications**:1-22 (2005).
3. Hasirci, V. and N. Hasirci, *Fundamentals of biomaterials*. 2018: Springer.
4. Al-Humairi, A.N.S., et al., *BIOMATERIALS: Multidisciplinary approaches and their related applications*. 2020: White Falcon Publishing.
5. Zhu, Y. and S.J. Kaskel, "*Comparison of the in vitro bioactivity and drug release property of mesoporous bioactive glasses (MBGs) and bioactive glasses (BGs) scaffolds"*. **Microporous Mesoporous Materials**, 118(1-3):176-182 (2009).
6. Greenwald, A.S., et al., "*Bone-graft substitutes: facts, fictions, and applications"*. **The Journal of Bone and Joint Surgery**, 83(2):S98-103 (2001).
7. Szpalski, M. and R.J. Gunzburg, "*Applications of calcium phosphate-based cancellous bone void fillers in trauma surgery"*. **Orthopedics**, 25(5):S601-S609 (2002).
8. Amini, A.R., C.T. Laurencin, and S.P.J. Nukavarapu, "*Bone tissue engineering: recent advances and challenges"*. **Critical Reviews™ in Biomedical Engineering**, 40(5) (2012).
9. Donos, N., X. Dereka, and E.J. Calciolari, "*The use of bioactive factors to enhance bone regeneration: A narrative review"*. **Journal of clinical periodontology**, 46:124-161 (2019).
10. Fleming, J.E., C.N. Cornell, and G.F.J. Muschler, "*Bone cells and matrices in orthopedic tissue engineering"*. **Orthopedic Clinics**, 31(3):357-374 (2000).
11. Brito, M.A., et al., "*Histological comparison between biphasic calcium phosphate and deproteinized bovine bone on critical-size bone defects"*. **Brazilian Dental Journal**, 32:26-33 (2021).

12. Rosen, P.S., M.A. Reynolds, and G.M.J. Bowers, "*The treatment of intrabony defects with bone grafts"*. **Periodontology**, 22:88-103 (2000).
13. Rosenberg, E. and L.F.J. Rose, "*Biologic and clinical considerations for autografts and allografts in periodontal regeneration therapy"*. **Dental clinics of North America**, 42(3):467-490 (1998).
14. Laurencin, C. and Y. Khan, *Bone graft substitute materials. Medicine. İnstant Access to the minds of medicine*. 2005.
15. Nandi, S., et al., "*Orthopaedic applications of bone graft & graft substitutes: a review"*. **Indian Journal of Medical Research**, 132(1):15-30 (2010).
16. Parizi, A.M., et al., "*Human platelet rich plasma plus Persian Gulf coral effects on experimental bone healing in rabbit model: radiological, histological, macroscopical and biomechanical evaluation"*. **Journal of Materials Science: Materials in Medicine**, 23:473-483 (2012).
17. Ceyhan, T., et al., "*Production and characterization of a glass-ceramic biomaterial and in vitro and in vivo evaluation of its biological effects"*. **Acta Orthopaedica et Traumatologica Turcica**, 41(4):307-313 (2007).
18. Brunner, T.J., W.J. Stark, and A.R.J. Boccaccini, *Nanoscale bioactive silicate glasses in biomedical applications*, in *Nanotechnologies for the Life Sciences*. 2009.
19. Hench, L.L.J., "*The story of Bioglass®"*. **Journal of Materials Science: Materials in Medicine**, 17(11):967-978 (2006).
20. Gosain, A.K., "*Bioactive glass for bone replacement in craniomaxillofacial reconstruction"*. **Plastic reconstructive surgery**, 114(2):590-593 (2004).
21. Silver, I.A., J. Deas, and M.J. Erecińska, "*Interactions of bioactive glasses with osteoblasts in vitro: effects of 45S5 Bioglass®, and 58S and 77S bioactive glasses on metabolism, intracellular ion concentrations and cell viability"*. **Biomaterials**, 22(2):175-185 (2001).
22. Anesi, A., et al., "*In-vivo evaluations of bone regenerative potential of two novel bioactive glasses"*. **Journal of Biomedical Materials Research Part A**, (2023).
23. Drago, L., M. Toscano, and M.J. Bottagisio, "*Recent evidence on bioactive glass antimicrobial and antibiofilm activity: a mini-review"*. **Materials**, 11(2):326 (2018).

24. Sudagidan, M.J., *Test of biomaterials in biological systems*. 2001: Bioengineering Izmir Institute of Technology.
25. Oonishi, H., et al., "*Particulate bioglass compared with hydroxyapatite as a bone graft substitute*". **Clinical Orthopaedics Related Research**, 334:316-325 (1997).
26. Macedo, N.L.d., et al., "*Bone defect regeneration with bioactive glass implantation in rats*". **Journal of Applied Oral Science**, 12:137-143 (2004).
27. Elshahat, A., et al., "*The use of Novabone and Norian in cranioplasty: A comparative study*". **Journal of craniofacial surgery**, 15(3):483-489 (2004).
28. Amato, M.M., et al., "*Use of bioglass for orbital volume augmentation in enophthalmos: a rabbit model (oryctolagus cuniculus)*". **Ophthalmic Plastic Reconstructive Surgery**, 19(6):455-465 (2003).
29. Jia, W., et al., "*Bioactive glass for large bone repair*". **Advanced healthcare materials**, 4(18):2842-2848 (2015).
30. Majhi, M., R. Pyare, and S.J. Singh, "*Studies on preparation and characterizations of CaO–Na2O–SiO2–P2O5 bioglass ceramics substituted with Al2O3, TiO2 and ZrO2*". **Journal of Biomaterials Tissue Engineering**, 2(2):154-169 (2012).
31. Deliormanli, A.J., "*In vitro assessment of degradation and mineralisation of V2O5 substituted borate bioactive glass scaffolds*". **Materials Technology**, 29(6):358-365 (2014).
32. El Damrawi, G., et al., "*Structural Investigations on Na2O-CaO-V2O5-SiO2 Bioglass Ceramics*". **British Journal of Applied Science Technology**, 16:1-9 (2016).
33. Baino, F., "*Bioceramics in ophthalmology*". **Acta biomaterialia**, 10(8):3372-3397 (2014).
34. Hench, L.L.J.J.o.M.S.M.i.M., "*The story of Bioglass®*". 17(11):967-978 (2006).
35. Dubok, V.A.J., "*Bioceramics—yesterday, today, tomorrow*". **Powder Metallurgy Metal Ceramics**, 39:381-394 (2000).
36. Baino, F. and C.J. Vitale-Brovarone, "*Three-dimensional glass-derived scaffolds for bone tissue engineering: current trends and forecasts for the*

future". **Journal of biomedical materials research Part A**, 97(4):514-535 (2011).

37. Nicolodi, L., E. Sjölander, and K.J.K.N.I. Olsson, "*Biocompatible Ceramics-An overview of applications and novel materials"*. **KTH Nov**:4-12 (2004).
38. Majdi, H.S., A. Saud, and M. Al-Mamoori. *A Novel Nanocomposite (SR/HA/-nZnO) Material for Medical Application*. in *4th International Conference on Nanotechnologies and Biomedical Engineering: Proceedings of ICNBME-2019, September 18-21, 2019, Chisinau, Moldova*. 2020. Springer.
39. Välimäki, V.-V. and H.T.J. Aro, "*Molecular basis for action of bioactive glasses as bone graft substitute"*. **Scandinavian journal of surgery**, 95(2):95-102 (2006).
40. Park, J. and J. Bronzino, *Biomaterials: Principles and Applications,* , ed. s. Edition. 2002: Crc Press.
41. Neo, M., et al., "*Ultrastructural study of the A-W GC-bone interface after long-term implantation in rat and human bone"*. **Journal of biomedical materials research**, 28(3):365-372 (1994).
42. Gentleman, E., et al., "*The effects of strontium-substituted bioactive glasses on osteoblasts and osteoclasts in vitro"*. **Biomaterials**, 31(14):3949-3956 (2010).
43. Rz, L.J., "*Properties of osteoconductive biomaterials: calcium phosphates"*. **Clin Orthop Relat Res**, 395:81-98 (2002).
44. Jaffe, W.L. and D.F.J. Scott, "*Current concepts review-total hip arthroplasty with hydroxyapatite-coated prostheses"*. **JBJS**, 78(12):1918-34 (1996).
45. Hench, L.L. and S.M. Best, *Ceramics, glasses, and glass-ceramics: basic principles*, in *Biomaterials Science*. 2013, Elsevier. p. 128-151.
46. Neuman, W.F. and M.W.J. Neuman, "*The chemical dynamics of bone mineral"*. **The chemical dynamics of bone mineral**, (1958).
47. Xynos, I.D., et al., "*Ionic products of bioactive glass dissolution increase proliferation of human osteoblasts and induce insulin-like growth factor II mRNA expression and protein synthesis"*. **Biochemical biophysical research communications**, 276(2):461-465 (2000).

48. Cortizo, A.M., et al., "*Osteogenic activity of vanadyl (IV)–ascorbate complex: Evaluation of its mechanism of action*". **The international journal of biochemistry cell biology**, 38(7):1171-1180 (2006).
49. Jain, R.K., et al., "*Engineering vascularized tissue*". **Nature biotechnology**, 23(7):821-823 (2005).
50. Beitzel, K., et al., "*US definitions, current use, and FDA stance on use of platelet-rich plasma in sports medicine*". **The journal of knee surgery**, 28(01):029-034 (2015).
51. Thompson, K.H. and C.J. Orvig, "*Boon and bane of metal ions in medicine*". **Science**, 300(5621):936-939 (2003).
52. Bauer, T.W. and G.F.J. Muschler, "*Bone graft materials: an overview of the basic science*". **Clinical Orthopaedics Related Research®**, 371:10-27 (2000).
53. Zreiqat, H., et al., "*Mechanisms of magnesium-stimulated adhesion of osteoblastic cells to commonly used orthopaedic implants*". **Journal of Biomedical Materials Research: An Official Journal of The Society for Biomaterials,**, 62(2):175-184 (2002).
54. Meunier, P., et al., "*Strontium ranelate: dose-dependent effects in established postmenopausal vertebral osteoporosis—a 2-year randomized placebo controlled trial*". **The Journal of Clinical Endocrinology Metabolism**, 87(5):2060-2066 (2002).
55. Damen, J. and J.J. Ten Cate, "*Silica-induced precipitation of calcium phosphate in the presence of inhibitors of hydroxyapatite formation*". **Journal of dental Research**, 71(3):453-457 (1992).
56. Kim, M.-H., et al., "*Silicon supplementation improves the bone mineral density of calcium-deficient ovariectomized rats by reducing bone resorption*". **Biological trace element research**, 128:239-247 (2009).
57. Yamaguchi, M.J., "*Role of zinc in bone formation and bone resorption*". **The Journal of Trace Elements in Experimental Medicine:** , 11(2-3):119-135 (1998).
58. Wang, W. and K.W.J. Yeung, "*Bone grafts and biomaterials substitutes for bone defect repair: A review*". **Bioactive materials**, 2(4):224-247 (2017).

59. Demirkıran, N. and A.J. Künkül, "*Dissolution kinetics of ulexite in perchloric acid solutions"*. **International Journal of Mineral Processing**, 83(1-2):76-80 (2007).

60. Bulutcu, A., C. Ertekin, and M.K.J. Celikoyan, "*Impurity control in the production of boric acid from colemanite in the presence of propionic acid"*. **Chemical Engineering Processing: Process Intensification**, 47(12):2270-2274 (2008).

61. Benkovic, S.J., et al., "*Identification of borinic esters as inhibitors of bacterial cell growth and bacterial methyltransferases, CcrM and MenH"*. **Journal of medicinal chemistry**, 48(23):7468-7476 (2005).

62. Bailey, P., et al., "*Boron-containing antibacterial agents: effects on growth and morphology of bacteria under various culture conditions"*. **Antimicrobial agents chemotherapy**, 17(4):549-553 (1980).

63. Seong, H.-S., J.-P. Kim, and S.-W.J. Ko, "*Preparing chito-oligosaccharides as antimicrobial agents for cotton"*. **Textile Research Journal**, 69(7):483-488 (1999).

64. Ibrahim, A., et al., *Antimicrobial agents for textiles: Types, mechanisms and analysis standards*. 2021: IntechOpen London, UK.

65. Aoyagi, T., et al., "*Controlling oxygen coordination and valence of network forming cations"*. **Scientific reports**, 10(1):1-12 (2020).

66. El-Damrawi, G., et al., "*Structural investigations on Na2O–CaO-V2O5-SiO2 bioglass ceramics"*. **British Journal of Applied Science Technology**, 16(3):1-9 (2016).

67. Scior, T., et al., "*Why antidiabetic vanadium complexes are not in the pipeline of "big pharma" drug research? A critical review"*. **Current medicinal chemistry**, 23(25):2874-2891 (2016).

68. Das, S., et al., "*Anti-angiogenic vanadium pentoxide nanoparticles for the treatment of melanoma and their in vivo toxicity study"*. **Nanoscale**, 12(14):7604-7621 (2020).

69. Oliveira, J., R. Correia, and M.J. Fernandes, "*Surface modifications of a glass and a glass-ceramic of the MgO-3CaO· P2O5-SiO2 system in a simulated body fluid"*. **Biomaterials**, 16(11):849-854 (1995).

70. Brinker, C.J. and G.W. Scherer, *Sol-gel science: the physics and chemistry of sol-gel processing*. 2013: Academic press.
71. Rahaman, M.N., et al., "*Bioactive glass in tissue engineering"*. **Acta biomaterialia**, 7(6):2355-2373 (2011).
72. Saud, A.N., E. Koç, and O. Özdemir, "*A novel strategy to synthesize bioactive glass based on the eutectic reaction of B2O3–K2O"*. **Ceramics International**, (2022).
73. Brochu, A.B., S.L. Craig, and W.M.J. Reichert, "*Self-healing biomaterials".* **Journal of Biomedical Materials Research Part A**, 96(2):492-506 (2011).
74. Bajammal, S.S., et al., "*The use of calcium phosphate bone cement in fracture treatment: a meta-analysis of randomized trials"*. **JBJS**, 90(6):1186-1196 (2008).
75. Ginebra, M., *Calcium phosphate bone cements*, in *Orthopaedic bone cements*. 2008, Elsevier. p. 206-230.
76. Larsson, S., *Clinical aspects of calcium phosphate bone cements*, in *Orthopaedic bone cements*. 2008, Elsevier. p. 377-400.
77. Webb, J. and R.J. Spencer, "*The role of polymethylmethacrylate bone cement in modern orthopaedic surgery"*. **The Journal of bone joint surgery. British volume**, 89(7):851-857 (2007).
78. Alfayez, E.S., *Synergizing angiogenesis and osteogenesis in a smart bone substitute*. 2016, King's College London.
79. Basgorenay, B., et al., "*Preparation, modification, and characterization of acrylic cements"*. **Journal of applied polymer science**, 99(6):3631-3637 (2006).
80. Deb, S. and G. Koller, *Acrylic bone cement: genesis and evolution*, in *Orthopaedic bone cements*. 2008, Elsevier. p. 167-182.
81. Kuehn, K.-D., W. Ege, and U.J. Gopp, "*Acrylic bone cements: composition and properties"*. **Orthopedic Clinics**, 36(1):17-28 (2005).
82. Niculescu, M., et al., *Evolution of Cementation Techniques and Bone Cements in Hip Arthroplasty*, in *Handbook of Bioceramics and Biocomposites*. 2016, Springer. p. 859-899.
83. Lasa, B.V., *Poly (methylmethacrylate) bone cement: chemical composition and chemistry*, in *Orthopaedic bone cements*. 2008, Elsevier. p. 183-205.

84. Zapata, M.E.V., C.D.G. Tovar, and J.H.M.J. Hernandez, "*The role of chitosan and graphene oxide in bioactive and antibacterial properties of acrylic bone cements"*. **Biomolecules**, 10(12):1616 (2020).

85. Forte, M.A., et al., "*Is poly (methyl methacrylate)(PMMA) a suitable substrate for ALD?: A Review"*. **Polymers**, 13(8):1346 (2021).

86. Iqbal, K. and D.J. Sun, "*Synthesis of nanoencapsulated Glauber's salt using PMMA shell and its application on cotton for thermoregulating effect"*. **Cellulose**, 25(3):2103-2113 (2018).

87. McKeen, L.W., *Plastics used in medical devices*, in *Handbook of polymer applications in medicine and medical devices*. 2014, Elsevier. p. 21-53.

88. Begum, S.A., A.V. Rane, and K. Kanny, *Applications of compatibilized polymer blends in automobile industry*, in *Compatibilization of polymer blends*. 2020, Elsevier. p. 563-593.

89. Knop, A. and L.A. Pilato, *Phenolic resins: chemistry, applications and performance*. 2013: Springer Science & Business Media.

90. Zaioncz, S., et al., "*Toughening of Epoxy Resin by Methyl Methacrylate/2-Ethylhexyl Acrylate Copolymers: The Effect of Copolymer Composition"*. **Macromolecular Materials Engineering**, 292(12):1263-1270 (2007).

91. Her, B., A. Jones, and J.W.J. Wollack, "*A three-step synthesis of benzoyl peroxide"*. **Journal of Chemical Education**, 91(9):1491-1494 (2014).

92. Dunnick, J.K., et al., "*Molecular changes in the nasal cavity after N, N-dimethyl-p-toluidine exposure"*. **Toxicologic pathology**, 44(6):835-847 (2016).

93. Modolo, L.V., et al., "*A minireview on what we have learned about urease inhibitors of agricultural interest since mid-2000s"*. **Journal of advanced research**, 13:29-37 (2018).

94. Dağlılar, S., et al., "*Mechanical Properties of Bioceramic Reinforced Bone Cement"*. **J Aust. Ceram. Soc**, 42(2):6-9 (2006).

95. Habraken, W., J. Wolke, and J.J. Jansen, "*Ceramic composites as matrices and scaffolds for drug delivery in tissue engineering"*. **Advanced drug delivery reviews**, 59(4-5):234-248 (2007).

96. Brunner, T.J., W.J. Stark, and A.R.J.P.X.L.o.C.X. Boccaccini, "*Nanoscale bioactive silicate glasses in biomedical applications"*. (2009).

97. Kokubo, T. and H. Takadama, "*How useful is SBF in predicting in vivo bone bioactivity?"*. **Biomaterials**, 27(15):2907-2915 (2006).

98. Chen, L., et al., "*Silicate bioceramic/PMMA composite bone cement with distinctive physicochemical and bioactive properties"*. **Rsc Advances**, 5(47):37314-37322 (2015).

99. Samad, H.A., et al., "*New bioactive glass-ceramic: Synthesis and application in PMMA bone cement composites"*. **Bio-medical materials engineering**, 21(4):247-258 (2011).

100. De Aza, P., F. Guitian, and S. De Aza, "*Bioactivity of wollastonite ceramics: in vitro evaluation"*. **Scripta metallurgica et materialia**, 31(8):1001-1005 (1994).

101. Goel, A., *Clinopyroxene based glasses and glass-ceramics for functional applications*. 2009, Universidade de Aveiro (Portugal).

102. Singh, R.K., G. Kothiyal, and A. Srinivasan, "*Bioactivity of CaO–SiO2–P2O5–Na2O–Fe2O3 glass-ceramics: in vitro evaluation"*. **Arch. Bioceram. Res**, 8:89-92 (2008).

103. Nayak, J., S. Kumar, and J. Bera, "*Sol–gel synthesis of bioglass-ceramics using rice husk ash as a source for silica and its characterization"*. **Journal of Non-Crystalline Solids**, 356(28-30):1447-1451 (2010).

104. Dhivya, V., et al., "*Role of TiO2 in modifying elastic moduli and enhancing in vitro bioactivity of fluorophosphate glasses"*. **Journal of Non-Crystalline Solids**, 608:122250 (2023).

105. Saud, A.N., E. Koç, and O. Özdemir, "*A novel strategy to synthesize bioactive glass based on the eutectic reaction of B2O3–K2O"*. **Ceramics International**, 49(6):9268-9278 (2023).

106. Magdas, D., N. Vedeanu, and D. Toloman, "*Study on the effect of vanadium oxide in calcium phosphate glasses by Raman, IR and UV–vis spectroscopy"*. **Journal of Non-Crystalline Solids**, 428:151-155 (2015).

107. Dhivya, V., et al., "*Effects of strontium-containing fluorophosphate glasses for enhancing bioactivity and enamel remineralization"*. **Materials Characterization**, 181:111496 (2021).

108. Yang, B., et al., *Vanadium: Extraction, manufacturing and applications*. 2020: Elsevier.

109. Dhivya, V., et al., "*Impact of silver on fluorophosphate glasses to improve in vitro bioactivity and antibacterial efficacy*". **Ceramics International**, 48(17):25346-25354 (2022).

110. Filho, O.P., G.P. La Torre, and L.L. Hench, "*Effect of crystallization on apatite-layer formation of bioactive glass 45S5*". **Journal of Biomedical Materials Research: An Official Journal of The Society for Biomaterials and The Japanese Society for Biomaterials**, 30(4):509-514 (1996).

111. Lenin, N., et al., "*Electrical, magnetic and structural properties of polymer-blended lanthanum-added nickel nano-ferrites*". **Ceramics International**, 44(17):21866-21873 (2018).

112. Kaur, G., et al., "*A review of bioactive glasses: their structure, properties, fabrication and apatite formation*". **Journal of Biomedical Materials Research Part A: An Official Journal of The Society for Biomaterials, The Japanese Society for Biomaterials, and The Australian Society for Biomaterials and the Korean Society for Biomaterials**, 102(1):254-274 (2014).

113. Chavan, C., et al., "*Ion dynamics and positron annihilation studies on polymer ceramic composite electrolyte system (PVA/NaClO4/Y2O3): Application in electrochemical devices*". **Ceramics International**, 48(12):17864-17884 (2022).

114. Utlak, S.A., *Modeling complex oxides: Thermochemical behavior of nepheline-forming Na-Al-Si-BK-Li-Ca-Mg-Fe-O and hollandite-forming Ba-Cs-Ti-Cr-Al-Fe-Ga-O systems*. 2019, University of South Carolina.

115. Jones, J.R., "*Review of bioactive glass: from Hench to hybrids*". **Acta biomaterialia**, 9(1):4457-4486 (2013).

116. Peitl, O., E.D. Zanotto, and L.L. Hench, "*Highly bioactive P2O5–Na2O–CaO–SiO2 glass-ceramics*". **Journal of Non-Crystalline Solids**, 292(1-3):115-126 (2001).

117. Hench, L.L., N. Roki, and M.B. Fenn, "*Bioactive glasses: Importance of structure and properties in bone regeneration*". **Journal of Molecular Structure**, 1073:24-30 (2014).

118. Dos Santos, V., R.N. Brandalise, and M. Savaris, *Engineering of biomaterials*. Vol. 10. 2017: Springer.

119. Boccaccini, A.R., et al., "*Sintering, crystallisation and biodegradation behaviour of Bioglass®-derived glass–ceramics*". **Faraday discussions**, 136:27-44 (2007).
120. El-Kady, A.M. and M.M. Farag, "*Bioactive glass nanoparticles as a new delivery system for sustained 5-fluorouracil release: characterization and evaluation of drug release mechanism*". **Journal of Nanomaterials**, 16(1):399-399 (2016).
121. Lefebvre, L., et al., "*Sintering behaviour of 45S5 bioactive glass*". **Acta biomaterialia**, 4(6):1894-1903 (2008).
122. Izquierdo-Barba, I., et al., "*High-performance mesoporous bioceramics mimicking bone mineralization*". **Chemistry of Materials**, 20(9):3191-3198 (2008).
123. Brauer, D.S., et al., "*Fluoride-containing bioactive glasses: effect of glass design and structure on degradation, pH and apatite formation in simulated body fluid*". **Acta Biomaterialia**, 6(8):3275-3282 (2010).
124. Huang, G., et al., "*A novel bioactive glass-based root canal sealer in endodontics*". **Journal of Dental Sciences**, 17(1):217-224 (2022).
125. Goto, K., et al., "*Mechanical, setting, and biological properties of bone cements containing micron-sized titania particles*". **Journal of Materials Science: Materials in Medicine**, 19:1009-1016 (2008).
126. Rentería-Zamarrón, D., et al., "*Mechanical properties and apatite-forming ability of PMMA bone cements*". **Materials Design**, 30(8):3318-3324 (2009).
127. Phakatkar, A.H., et al., "*Novel PMMA bone cement nanocomposites containing magnesium phosphate nanosheets and hydroxyapatite nanofibers*". **Materials Science Engineering: C**, 109:110497 (2020).
128. Serbetci, K., F. Korkusuz, and N.J. Hasirci, "*Thermal and mechanical properties of hydroxyapatite impregnated acrylic bone cements*". **Polymer Testing**, 23(2):145-155 (2004).
129. Roemhildt, M., S. Wagner, and T.J. McGee, "*Characterization of a novel calcium phosphate composite bone cement: flow, setting, and aging properties*". **Journal of Materials Science: Materials in Medicine**, 17:1127-1132 (2006).

130. Richardson, I.J., "*The nature of the hydration products in hardened cement pastes"*. **Cement Concrete Composites**, 22(2):97-113 (2000).
131. Liu, W., et al., "*Novel tricalcium silicate/magnesium phosphate composite bone cement having high compressive strength, in vitro bioactivity and cytocompatibility"*. **Acta biomaterialia**, 21:217-227 (2015).
132. Costantino, P.D., et al., "*Applications of fast-setting hydroxyapatite cement: cranioplasty"*. **Otolaryngology—Head Neck Surgery**, 123(4):409-412 (2000).
133. Miola, M., G. Lucchetta, and E.J. Verné, "*Physical, Mechanical, and Biological Properties of PMMA-Based Composite Bone Cement Containing Silver-Doped Bioactive and Antibacterial Glass Particles with Different Particles Sizes"*. **Materials**, 16(13):4499 (2023).
134. Jasso-Gastinel, C.F., et al. *Acrylic bone cements modified with bioactive filler*. in *Macromolecular symposia*. 2009. Wiley Online Library.
135. Lewis, G.J., "*Properties of acrylic bone cement: state of the art review"*. **Journal of biomedical materials research**, 38(2):155-182 (1997).

RESUME

Anmar Fouad Kadhim IBADI is a material engineer who graduated from the Faculty ofmaterials Engineering, University of Babylon - Iraq. He received His Bachelor’s degree in 2018. He is currently studying for her Master's degree at Karabük University in the field of Materials Engineering.